Detection and sorting of micro-beads and bacteriophages in a microfluidic biochip

Beno Hendrik Kunst

Promotoren:

Prof. dr. A.J.W.G. Visser
Hoogleraar Biochemische Microspectroscopie
Wageningen Universiteit

Prof. dr. S.C de Vries
Hoogleraar Biochemie
Wageningen Universiteit

Copromotor:

Dr. ir. A. Schots
Universitair docent
Laboratorium voor Moleculaire Herkenning en
Antilichaam Technologie

Promotiecommisie:

Prof. dr. ir. A. van den Berg, Universiteit Twente
Prof. dr. E.J.R. Sudholter, Wageningen Universiteit
Prof. dr. M.A. Cohen Stuart, Wageningen Universiteit
Prof. dr. R.M. Boom, Wageningen Universiteit

Detection and sorting of micro-beads and bacteriophages in a microfluidic biochip

Beno Hendrik Kunst

Proefschrift
ter verkrijging van de graad van doctor
op gezag van de rector magnificus
van Wageningen Universiteit,
Prof. dr. M.J. Kropff
in het openbaar te verdedigen
op dinsdag 28 november 2006
des namiddags te half twee in de Aula

Detection and sorting of micro-beads and bacteriophages in a microfluidic biochip

Kunst, Beno Hendrik

Thesis Wageningen University, The Netherlands
With references – with summary in Dutch

ISBN: 90-8504-563-0

Contents

Chapter 1

Introduction

Fluorescence microscopy, protein interactions and microfluidics

A continuing challenge in biomolecular research is the capacity to monitor cellular and molecular processes in real time and in the context of a living cell or organism. The ultimate goal is to visualize single biological molecules like proteins and their interactions *in vivo*. The advent of fluorescent proteins and specific fluorescent probes has facilitated the rapid development of modern fluorescence microscopy to measure protein-protein interactions in a quantitative way. In addition, fluorescence microscopy techniques offer the possibility for analytical measurement of several cellular parameters such as pH, ion concentrations such as calcium, membrane potentials, molecular transport, diffusion and velocity and many more. A drawback in fluorescence microscopy is the optical resolution limit, which is for the best cases 500-800 nm along the optical axis and 180 nm in the focal plane (Hell, 2003). New technologies are required to enhance the spatial resolution, as the resolution is inadequate to study, for instance, the detailed 3D architecture of cell organelles. Recent novel technologies such as 4Pi confocal microscopy and stimulated emission depletion (STED) microscopy have provided the first evidence for resolution improvement down to 28 nm (Hell, 2003). However, to make fluorescence microscopy a really accessible and versatile research tool it is necessary to continuously develop new types of techniques and instrumentation in many collaborating fields. We need chemistry for novel probe and sensor development, molecular biology for expression of novel fluorescent proteins, micro-mechanical engineering for construction of microfluidic devices, spectroscopy for obtaining better optical contrast in microscopy, computing and software development for process control and data analysis.

Most cellular activities require the integrated functioning of a multitude of different proteins organised into protein complexes. In many biochemically well-documented cases proteins closely work in concert due to the presence of multi-protein networks. Examples are diverse signal transduction pathways, metabolic routes, transcriptional complexes and biosynthetic pathways. Identification of interacting proteins with a given protein of interest is therefore

an important aspect of current biochemistry. The completion of several large genome projects and the development of high-throughput technologies, such as metabolomics, transcriptomics and proteomics, have resulted in a comprehensive array of tools, resources and information being readily available for researchers to use. In this era of functional genomics the development of new methods for the screening of bio-libraries for proteins binding to ligands including the presence of other proteins is of increasing importance. High-throughput screening strategies are preferred in this respect as they allow screening of large numbers in a micro setting. In this thesis experiments are described that are directed to the screening of bio-libraries. The principle is based on the detection of fluorescent particles in a flow in microfluidic chips (biochips). These biochips have been designed and produced. The biochip can be mounted on the stage of a confocal fluorescence microscope that has the capacity to measure the fluorescence of single molecules. When a fluorescent particle in a flow is entering the confocal volume, a burst of fluorescent photons is generated and detected. After burst detection it is then possible to direct the flow into another channel and in this way sort the particle. The biochips allow screening of various types of libraries such as phage-based libraries, micro-organisms expressing proteins or protein coated microspheres. The system has the advantage that it prevents cross-contamination. The choice for the combination of a microfluidics-microscopy system was made, because numerous parallel devices could be designed, which would enhance the rate of screening and allow a precise selection of binders at relatively high speed.

One of the first micro Fluorescence Activated Cell Sorters (μFACS) was built by the group of Stephen Quake (Fu *et al.*, 1999). They successfully sorted fluorescent micro-beads and fluorescent *E.coli* cells using electrokinetic flow. The sorting speed was between 1 and 40 cells per second (Fu *et al.*, 2002). Applegate and coworkers (2006) used an integrated optical platform to optically trap and guide particles and detect their fluorescence using waveguides. The latter authors claim that their approach streamlines microfluidic sorting and minimizes optical complexity commonly associated with external platforms. Particles of 4 μm size could be sorted with a speed of 5 particles per second. For an overview of microfluidic sorters see Andersson and van den Berg, (2003).

The aim of the following section is to provide an overview of most current procedures for detecting protein interactions as a backdrop for the research carried out in this thesis.

Screening methods

There is a wide variety in methods available to isolate interacting proteins or peptides or to verify interactions found in other *in vivo* screens. Here only the most common ones will be mentioned.

1. Phage display screens use modified phage vectors to express proteins on the surface of the viral coat particles. After production and lysis of host cells the resulting interactions can be followed using antibodies or purified proteins to detect those virus particles that express a given protein fusion of interest (expand). Although this procedure worked, it is quite tedious, requires a lot of rounds of purification and eventually is known to generate a large number of false positives that need to be removed by other methods such as ELISA (see below). The advantage of phage display screening is the ability to also use non-proteinacious molecules as "bait", but it is not easy to get to work in a semi-automated environment (Bradbury *et al.*, 2003; de Wildt *et al.*, 2000). One additional problem is that interactions take place *in vitro*, outside of their normal environment and therefore may not represent true interactions inside the cell.

2. Yeast interaction screening was one of the first working methods to overcome some of these limitations and was designed to identify interacting proteins inside a living yeast cell. The method uses proteins encoded in a so-called bait vector where it is expressed as part of a fusion protein with the DNA-binding domain of the lexA repressor. Upon binding to a candidate interacting protein that is expressed from a second vector that makes use of a fusion protein between the cDNA library of the organism of interest and the lexA activator domainA, the resulting complete lexA repressor then moves into the yeast nucleus to start transcription from a promoter-reporter construct using the lacZ protein. Additional selection systems present in the vectors confer autotrophy to the host strains. Recent modifications are methods that employ membrane-localized reporters or require three interacting partners (Drees, 1999; Licitra and Liu, 1996). Also yeast screening, at least for those working with other organisms, can give a lot of false positives due to the required interaction in the yeast nucleus or simply do not show interactors since they were not present in the cDNA library used for screening (de Wildt *et al.*, 2000; van Criekinge and Beyaert, 1999).

3. A method that is currently widely used employs mass spectrometry of proteins in a mixture that are interacting with a tagged version of a given protein. Protein tags can be short natural or artificial polypeptides that have been added to the protein of interest before re-introduction into the cell. Common procedures involve tandem-affinity purification (TAP) tags to reduce false positives (Rigaut *et al.*, 1999). Ideally it must be ascertained that the introduction of these short tags does not interfere with the normal functioning of the protein when possible by genetic complementation of a mutation in the corresponding gene, but this is not always practical or possible. Although this method is more likely to identify true interactors in the cells under investigation, greatest care must be taken to ensure that during the cellular disruption and subsequent procedures no artefacts have been introduced. When care is taken, this is the most reliable method to date to isolate interacting proteins from cells (Butland *et al.*, 2005; Gavin *et al.*, 2002; Rigaut *et al.*, 1999; Suter *et al.*, 2006).

   There are a number of *in vitro* methods available that are commonly used to verify interactions once they have been identified in screens.

4. Enzyme Linked Immuno Sorbent Assays (ELISA), a method whereby a ligand or protein is immobilized on the surface of a 96-well plate and interaction with single proteins or proteins present in cell lysates is measured by an enzyme linked to an antibody that detects the bound protein is widely used in research to detect the presence of antigens or antibodies (Bradbury *et al.*, 2003). Other sensitive and versatile methods are *e.g.* BIACORE where interaction is determined using surface plasmon resonance (SPR). Here, not only interaction, but also association and disassociation as well as true interaction kinetics can be determined. The methods can be used for determining one-to-one interactions or can also be adapted for genome-wide screening methods. In most cases no prior labelling or modification of proteins is required, but they have not been as popular today as yeast-based methods.

5. Pull-down assays. Traditional *in vitro* methods are based on disruption of cells followed by isolation of a protein of choice via a variety of purification methods. This way copurifying proteins often have been found that turned out to be important regulators of the enzyme under investigation (Suter *et al.*, 2006). Success or failure depends mainly on the strength of the interaction and the protocols used. Currently pull-down assays, where one

protein is immobilized on beads and used to retain other purified proteins or mixtures of proteins up to entire cell lysates are used to verify other methods. While quick and often useful to determine other parameters determining interaction, such as phosphorylation, the methods operate completely outside of a cellular context and require cloning and expression of often-tagged proteins in suitable hosts as well as the availability of specific antibodies. Many variants such as blot-immobilized proteins are available and their usage depend on the type of proteins under investigation. In general, these methods are useful as a back up of studies where genetic interactions have been shown or where other large-scale interaction screens have been used (Arifuzzaman *et al.*, 2006).

6. Co-immunoprecipitation often employing tagged proteins to ensure specificity is the traditional way of verifying interactions *in vivo*. Briefly, tagged proteins are collected by means of any affinity procedure available, using specific anti-tag antibodies. After precipitation the proteins are collected and challenged with an antibody against the presumed interacting protein. In principle the effect of other molecules such as ligands on the interaction properties can be determined this way. No information in general is obtained on the precise localisation in the cell of the interactions.

In silico methods

7. Vast databases are now available detailing the interactomers of *e.g.* yeast, fruit fly, worms and many other organisms. Mostly a variety of methods are being used to construct such databases. The most prominent ones are being based on yeast interaction screens and MS-based methods as well as on genetic and phenotypical data (Gandhi *et al.*, 2006) (Human protein reference database: www.hprd.org).

8. Prediction of interacting partners solely using 3D models is not really possible at present, but when based on available information can give predictive tools to help set up real experiments. For example motif-based databases can predict fairly accurately whether there is a good chance of finding an interaction with a protein docking on such a peptide motif. This method is often used in heterologous systems and can be quite useful in selecting candidate genes for further experiments (Balla *et al.*, 2006; El Karkouri *et al.*, 2005) (www.ebi.ac.uk/Tools).

Verification and examples

Whatever starting point is being used for a screen to identify interacting proteins (*e.g.* a genetic screen for a particular phenotype or a given single protein) there will always be the need for verification methods using a completely different approach. In case of a genetic interaction this could be a pull-down assay or yeast interaction, in case of a protein complex isolated by immunological methods and protein identification by MS this may be a demonstration of a genetic interaction.

In yeast the entire proteome has been subjected to interaction screening and mass spectrometry on co-immunoprecipitated complexes (www.yeastgenome.org, tap.med.utoronto.ca). It appeared that there were very large differences between the numbers of interacting proteins. Some are clearly hotspots while others have only one or two or sometimes no interacting partners (Gavin *et al.*, 2006; Krogan *et al.*, 2006). A comparison of these methods recently pointed out the difficulties and problems associated with such large-scale projects. In yeast it is assumed that approximately 800 so-called "core" machines exist that contain the same proteins, no matter which protein was used as a tag or which purification procedure was used (Gavin *et al.*, 2006). However, substantial differences were detected even between repetitive isolations of the same complexes, while also differences exist between the same protein in different experiments or in different conditions; part of this being due to the fact that a given protein can be part of different complexes that or apparently not always assembles. Also a lot of proteins appear to be only loosely attached, possibly representing modulators of complex activity. When compared with earlier experiments using different tags and only subsets of the yeast proteome, the number of proteins found to be in common between the corresponding tags that were used in initial studies, only about 9% of the proteins were found in all studies (Goll and Uetz, 2006). Earlier work had used extensive yeast interaction screens. In these screens, protein-protein interactions were compared one-by one and appeared to detect more transient protein interactions rather then the more stable protein interactions found by the immunoprecipitation/MS based methods. Problems arose when attempting to integrate gene expression profiles such as obtained from DNA micro array experiments and proteomic analyses. In most cases there seems to be very little direct correspondence between both.

For multicellular organisms these interaction maps, now available for yeast, are further complicated due to the different cell types that make

up the organ or group of cells under investigation. Recently Gandhi *et al*. (2006) compared databases containing protein-protein interaction (PPI) data from yeast and multicellular organisms including humans. This represents the first attempt to describe a human interactome and relies on the assumption that orthologue protein pairs interacting in one organism are expected to do the same in another one. Surprisingly, only 42 interactions out of a total of more then 70,000 interaction pairs were shared between all, mainly involved in basic processes such as DNA replication or RNA maturation. There was no correlation between the number of interacting proteins and the essentiality of the genes as inferred from knockout studies. One correlation was noted in which genes known to result in general disorders also showed direct interactions, suggesting that the genes resulting in the same detectable phenotype have a high chance of being in the same protein complex. Few of the present studies on multicellular organisms take into account that proteins may change not only their subcellular location but may also be transported to different cells or even different organs.

In plants only few examples have been published that point out the importance of the existence of large sets of protein complexes. Systematic yeast interaction screens done for the MADS box family of transcription factors showed parallels to work in animal cells in that certain members of this family are found to be able to interact with different partners, often involved in the same developmental process, while others are very rare interactors (de Folter *et al.*, 2005). Recently Karlova *et al.* (2006) isolated a membrane receptor complex by co-immunoprecipitation in which at least several proteins were present that were also found in previous yeast interaction screens as well as in genetic screens, thus providing solid evidence for the existence *in vivo* of this apparently functional receptor complex.

Finally, one of the biggest challenges will be to visualize protein interactions and corresponding changes in activity and subcellular location in real time *in vivo*. Methods based on genetics, MS, bioinformatics and on fluorescence microspectroscopy are indispensable to achieve these goals that is now commonly referred to as a systems biology approach where information from many different levels and experimental procedures are combined in interactive databases.

Outline of this thesis

As a prerequisite for proper development of the biochip system, the flow of fluorescent molecules and particles in a commercially available micro-capillary has been studied using fluorescence correlation spectroscopy. These experiments are described in **chapter 2**. The principle is based on the passage of flowing particles through the confocal volume element that results in excitation and generation of fluorescence photons that are detected through confocal optics by an avalanche photodiode. The fluctuating intensities of the fluorescence are autocorrelated in real time by a hardware correlator. The flow rate of a fluorescent particle in the capillary is determined by fitting the autocorrelation traces with a model containing the flow-rate as one of the parameters. It was found that optical forces generated by increasing laser beam intensities retard the flow of larger particles and bacteria.

Chapter 3 is based on a minireview discussing the current achievements in generating biolibraries, single-molecule fluorescence detection techniques and microfluidic devices. The selection of specific binding molecules like peptides and proteins from biolibraries using, for instance, phage display methods can be quite time-consuming. It is therefore desirable to develop a strategy that is much faster in selection and sorting of potential binders out of a biolibrary. A high-throughput microfluidic prototype platform is then proposed that combines the propulsion of liquid containing fluorescent components of the biolibrary through microchannels, single-molecule fluorescence photon burst detection and real-time sorting of positive hits.

In **chapter 4** a microfluidic system is described that is capable of detecting and sorting single fluorescent particles. The system consists of microfluidic chips (biochips), computer controlled high voltage power supplies, and a fluorescence microscope with confocal optics. In this chapter and in supplementary material the detection and real-time sorting of (strongly) fluorescent microspheres are demonstrated. Based on supplementary experiments the limitations of these biochips for screening of fluorescent bacteriophages are briefly discussed.

In **chapter 5** the most important results are summarized and some future perspectives are given.

Chapter 2

Detection of flowing fluorescent particles in a micro-capillary using fluorescence correlation spectroscopy.

Capillary flow experiments are described with fluorescent molecules, bacteria and microspheres using fluorescence correlation spectroscopy as an analytical tool. The flow velocity in the microcapillary is determined by fitting autocorrelation traces with a model containing parameters related to diffusion and flow. The flow profile of pressure-driven flow inside a microcapillary is determined using the fluorescence fluctuations of a small dye molecule. It was found that bacteria and microspheres are retarded in their flow by optical forces produced by the laser beam.

This chapter has been published as:

B.H. Kunst, A. Schots and A.J.W.G. Visser
Analytical Chemistry, 2002, **74**, 5350-5357.

Introduction

The ability of screening particles is becoming more important in the fields of drug discovery and functional genomics. The groups of Eigen and Rigler have pioneered (Dörre *et al.*, 1997; Eigen and Rigler, 1994; Oehlenschläger *et al.*, 1996; Rigler, 1995) high throughput screening based on sensitive fluorescence detection methods and an increasing number of applications are currently under development in the pharmaceutical industry (de Wildt *et al.*, 2000; Hertzberg and Pope, 2000; Pope *et al.*, 1999; Rudiger *et al.*, 2001; Wölke and Ullmann, 2001). Several groups reported detection of single molecules in microstructures using confocal detection schemes (Dörre *et al.*, 2001; Gösch *et al.*, 2000; Lee *et al.*, 1994; Lyon and Nie, 1997; Mathis *et al.*, 1997; Nie *et al.*, 1995; Zander *et al.*, 1998) or recently in submicron structures (Foquet *et al.*, 2002). Here a feasibility study is described to detect flowing, single fluorescent particles and fluorescent microorganisms in a micro-fluidic setup. This strategy fulfills a basic prerequisite for more complex applications such as screening of complex bio-libraries with fluorescent ligands (Georgiou, 2001; Georgiou *et al.*, 1996; Schwalbach *et al.*, 2000; Stathopoulos *et al.*, 1996).

Antibody libraries are the clearest example of biolibraries. They are widely used today, to select for antibodies used in research and diagnosis and for applications in human medicine. These libraries comprise a large number (up to $>10^{10}$) different antibody fragments. Other examples of biolibraries are peptide libraries, cDNA libraries and libraries used to select for protein variants suited for specific applications. Examples of the latter comprise protease inhibitors, proteases, β-lactamase, lipases etc. Most bio-libraries are displayed on bacteriophage, bacteria and yeast cells and consist often of $>10^{8}$ genetically different variants. Selection usually involves several rounds wherein complexed ligands are captured batch wise followed by amplification in a bacterial host. After the last selection round, the remaining binders often have improved characteristics. An important drawback of display systems is the low specificity of the batch wise selection strategies and the necessary amplification step may result in a loss of interesting binders as a consequence of genetic instability. To improve selection it is necessary to enable specific detection. The advantages are paramount; fast and specific selection as well as a reduced loss of genetic diversity compared to the conventional methods. Required is a method to detect single complexes followed by selective extraction. This single particle detection and sorting can be carried out using narrow channels in microfluidic biochips. However, before this methodology can be applied, it is necessary to

understand the movement of macroscopic particles through the microchannels and to design detection and sorting strategies of fluorescent binders.

Therefore we report on experiments with single fluorescent particles in a flowing liquid, with an emphasis on the possibilities to detect these particles using confocal detection methods in particular fluorescence correlation spectroscopy (FCS) (Aragón and Pecora, 1975, 1976; Ehrenberg and Rigler, 1974, 1976; Elson and Magde, 1974; Gösch *et al.*, 2000; Koltermann *et al.*, 1998; Magde *et al.*, 1974; Magde *et al.*, 1978; Rigler *et al.*, 1993; Thompson, 1991; Widengren *et al.*, 1995; Winkler *et al.*, 1999), as well as their movement through microcapillaries. These particles are used as a model for the detection of fluorescent ligand-receptor complexes, on bacteriophages, microspheres, bacteria or yeast cells, which is based on fluorescence photon bursts upon passage through the confocal excitation volume.

Different fluorescent systems varying in size from small fluorescent molecules to intrinsically fluorescent *Escherichia coli* bacteria and macroscopic fluorescent microspheres were used in this study. In FCS, fluctuations in the fluorescence signal due to passage of single molecules through the Confocal Volume Element (CVE) are detected. Because of the small volume involved (approximately one femtoliter) background emission is largely reduced and therefore only photons emitted by single fluorophores excited in the CVE are detected. Due to the microscope optics only a small fraction (circa 3%) of emitted photons is detected. The fluctuations in fluorescence intensities are autocorrelated yielding information about the number of fluorescent particles, diffusion properties and chemical kinetics. Not only the autocorrelation traces, but also the time window of the individual photons contain information about the fluorescent molecules such as number and brightness (Chen *et al.*, 1999; Enderlein and Kollner, 1998; Kask *et al.*, 1997; Kask *et al.*, 2000; Kask *et al.*, 1999; Widengren *et al.*, 1995). The obtained results contribute to the development of a system allowing specific and rapid detection and selection of binders from bio-libraries.

Materials and Methods

Theoretical background

Since flowing single fluorescent molecules are detected, the real-time autocorrelation of the fluorescence intensity fluctuations is used for the analysis of diffusion and flow. The diffusion rate can be determined by auto-correlating

numerous photon events. The theoretical framework for applications of FCS in the analysis of uniform translation (plug flow) and laminar flow, superimposed on diffusion and active transport has been given by Magde *et al.* (1978). Let us briefly summarize the expressions for the auto-correlation function describing diffusion only. Assuming a Gaussian detection volume, the auto-correlation function $G(\tau)$ can be written as (Widengren and Rigler, 1998):

$$G(\tau) = 1 + \frac{1}{N} \cdot A$$

where

$$A = \left(1 + \frac{\tau}{\tau_{diff}} \right)^{-1} \cdot \left[1 + \left(\frac{\omega_{xy}}{\omega_z} \right)^2 \cdot \left(\frac{\tau}{\tau_{diff}} \right) \right]^{-\frac{1}{2}} \qquad (2\text{-}1)$$

Here N denotes the number of fluorescent particles, τ_{diff} is the diffusion time of the fluorescent particle (or its residence time in the CVE), ω_{xy} and ω_z are the radius and length of the CVE, respectively, assuming that the spatial intensity distribution of the laser beam has a Gaussian 3D-profile. The structure parameter, ω_z/ω_{xy}, is of importance since it reflects the optical quality of the CVE. It usually amounts to 5-10 for aqueous samples in chambers separated by a flat borosilicate bottom. The translational diffusion constant D_{trans} is related to the diffusion time τ_{diff}:

$$D_{trans} = \frac{\omega_{xy}^2}{4 \cdot \tau_{diff}} \qquad (2\text{-}2)$$

The recorded autocorrelation curves are analyzed using in-house developed global analysis software. In order to determine the structure parameter the dye Rhodamine Green was used for calibration because of its well determined (Magde *et al.*, 1974; Rigler *et al.*, 1991) D_{trans} of 2.8×10^{-10} $m^2.s^{-1}$. τ_{diff} and ω_z/ω_{xy} were obtained by fitting the autocorrelation data curves to Eq. 2-1, whereas the square of the beam waist, ω^2_{xy}, was obtained from Eq. 2-2.

The volume of the confocal volume element (V_{CVE}) can be estimated from:

$$V_{CVE} = \pi \omega_{xy}^2 \omega_z \tag{2-3}$$

When there is active transport in the form of laminar flow, the autocorrelation function $G(\tau)$ changes to (Brinkmeier *et al.*, 1999; Brinkmeier and Rigler, 1995; Gösch *et al.*, 2000):

$$G(\tau) = 1 + \frac{1}{N} \cdot e^{-\left[\left(\frac{\tau}{\tau_{flow}}\right)^2 \cdot A\right]} \tag{2-4}$$

where τ_{flow} is the average flow time of the fluorescent particles through the detection volume. In the following we refer to Eq. 2-4 as the fcs-flow model. The flow velocity v is given by:

$$v = \frac{\omega_{xy}}{\tau_{flow}} \tag{2-5}$$

The minimum flow velocity that can be measured is determined by Brownian diffusion. When the flow velocity is too small, it becomes difficult to distinguish between diffusion alone and diffusion superimposed on flow. Therefore, τ_{flow} must be distinctly shorter than the diffusion time, τ_{diff}, in order to recover the flow velocity from the analysis.

Setup

The experimental apparatus is built around a ConfoCor™ I (Carl Zeiss, Jena, Germany), an inverted confocal fluorescence microscope, especially designed to perform fluorescence correlation spectroscopy (Hink *et al.*, 1999). We used the 488 nm or 514 nm laser lines from an argon laser to excite, respectively, Enhanced Green Fluorescent Protein (EGFP) (Tsien, 1998), microspheres and Enhanced Yellow Fluorescent Protein (EYFP) (Tsien, 1998) in *E. coli*. A Zeiss 40 x 1.2 NA water immersion objective focuses the laser beam into a diffraction-limited spot. Neutral density filters were used to decrease the incident laser power (Visser and Hink, 1999). Usually a 96-well plate with borosilicate bottom (Whatman, Clifton, NJ, USA) is used to contain the samples. In this work a 100 x 100 μm^2 silica microcapillary (Polymicro Technologies Inc, Phoenix, USA) is used and mounted so that the laser spot (CVE) is located exactly in the middle of the capillary. Fluorescence photons emitted in the laser spot are detected by an avalanche photodiode (APD) (EG&G, Quebec, Canada) and autocorrelated in real time using an ALV-5000 autocorrelator card (ALV, Langen, Germany) in a Windows™ computer. We used the ConfoCor I software to control this card and to store the processed data. A digital storage scope (Agilent Technologies, Palo Alto, Ca, USA) has been used to observe the photon stream. With this instrument we observed that photons are converted by the APD to TTL pulses lasting 50 ns.

The capillary is connected via Valco connectors (Valco Instruments, Houston, TX, USA) to an injection system (Valve V7, Pharmacia, Uppsala, Sweden) and a standard FPLC pump (P-500, Pharmacia LKB, Uppsala, Sweden). With this system, samples (typically 0.025 - 2 ml, depending on the sample loop) can be injected in the flow of buffer (flow rate typically less than 5 $ml.h^{-1}$). A 1:3 flow splitter was used to obtain lower flow rates than the pump could deliver. The applied flow rate was measured through weighing of the pumped volume. The capillary fibre is coated with polyimide, which is of importance for the mechanical stability of the glass capillary. Prior to positioning the capillary on top of the objective, the coating was burnt off with a moderate flame (circa 1 cm). Cleaning of the fibre with soft tissue resulted in a surface of good optical quality.

Used reagents

Rhodamine Green, Rhodamine 6G and Green-Yellow fluorescent microspheres were obtained from Molecular Probes, Leiden, The Netherlands.

Fluorescent bacteria preparation

The open reading frame of EYFP cDNA was amplified by the polymerase chain reaction (PCR) from EYFP full length cDNA and was cloned into a pTYB11 vector (New England Biolabs, Impact vector system) using the following primers: YFPfor (5' GGTGGTTGCTCTTCCAACATGGTGAGCAAGGGCG 3') and YFPrev (5' GGTGGTGGATTCTTACTTGTACAGCTCG 3'). The pTYB11-EYFP construct was introduced into the BL21 DE3 *E. coli* bacteria strain for high expression levels. The cells were induced by adding 0.3 mM IPTG and grown at 20 ºC. The cells were harvested after 3 hours of induction and washed with buffer (50 mM Tris pH 8, 120 mM KCl and 15 % glycerol). Similar procedures using an open reading frame of EGFP full length cDNA yielded *E. coli* harbouring EGFP. The *E. coli*-EYFP (and *E. coli*-EGFP) cells were stored at –80 ºC. EYFP and EGFP were obtained as described recently (Griep *et al.*, 1999; Visser *et al.*, 2002).

Results and Discussion

Calibration

Calibration of the optical system was performed using 5 nM Rhodamine Green introduced in the capillary. The parameters obtained were used to calculate the radius and height of the detected confocal volume element and the structure parameter (see Eqs. 2-2 and 2-3). The confocal laser spot (laser light: 488 nm) was focused in the middle of the capillary. First the position of the 40 μm pinhole in the instrument was optimized using an automated procedure. Next, five autocorrelation curves collected during one minute per curve were obtained. Using these curves, the structure parameter of this setup was determined using Eqs. 2-1 and 2-2. Typically, Rhodamine Green gave a diffusion time of 90 μs, and a structure parameter of 15 resulting in a CVE of approximately 1.5 femtoliter (beam waist $\omega_{xy} \approx 320$ nm). The square capillary gave structure parameters that are about twice as large as usually found by using multiwell plates. This discrepancy was attributed to the less perfect optical quality of the capillary fibre. Multiwell plates contain borosilicate glass sheets, which have a much better flatness.

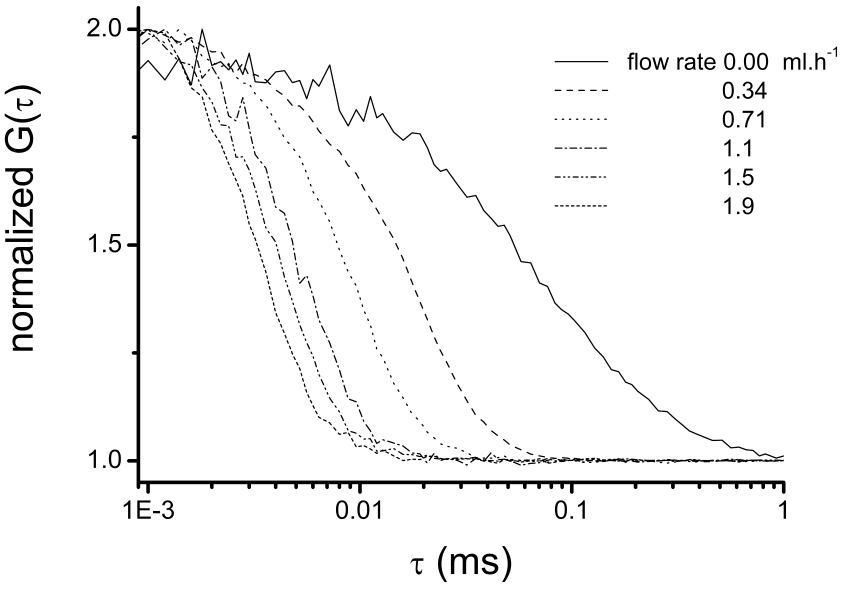

Figure 2-1. Normalized autocorrelation traces of 5 nM Rhodamine Green in water at different flow-rates.

The autocorrelation curve was measured using different pump speeds (see Figure 2-1). The diffusion time was fixed in the fcs-flow model (Eq. 2-4) to determine the flow velocities (Eq. 2-5) in the capillary from flow experiments with Rhodamine Green. We then fitted the experimental autocorrelation traces to the fcs-flow model and obtained, a linear correlation between the pump settings and the recovered flow velocity (see Figure 2-2).

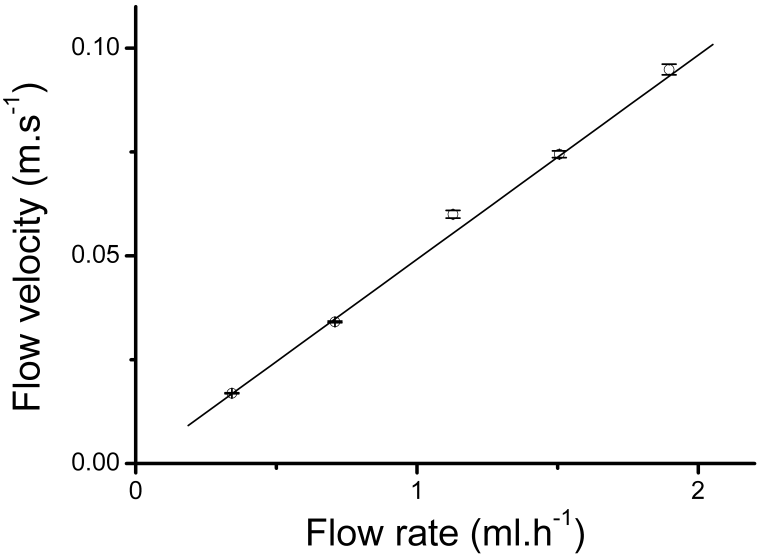

Figure 2-2. Flow velocities recovered from analysis with the fcs-flow model are linear with the applied flow rate through the capillary.

Flow profile in capillary

For flow profiling in the capillary we followed the procedure outlined by Gösch *et al.*, (2000). 2.5 nM Rhodamine Green was used as indicator dye and the lowest possible pump speed setting of 1 $ml.h^{-1}$ (without splitter) was applied. The diffraction limited laser spot was first focused in the middle of the capillary and spatially scanned through the width of the capillary with steps of 10 μm. The flow velocity was obtained by global fitting of several one-minute long autocorrelation curves to the fcs-flow model. The recovered flow velocity of the liquid in the middle of the 100 x 100 μm^2 capillary was around $5x10^{-2}$ $m.s^{-1}$ when the pump speed was set to its lowest value of 1 $ml.h^{-1}$. Using the recovered flow velocity the apparent residence time of a single, flowing Rhodamine Green molecule in the CVE (assuming a diameter of twice the beam waste) is then circa 13 μs. The recovered flow velocity is comparable to the average flow velocity that can be calculated from the pump speed and the geometry of the capillary fibre.

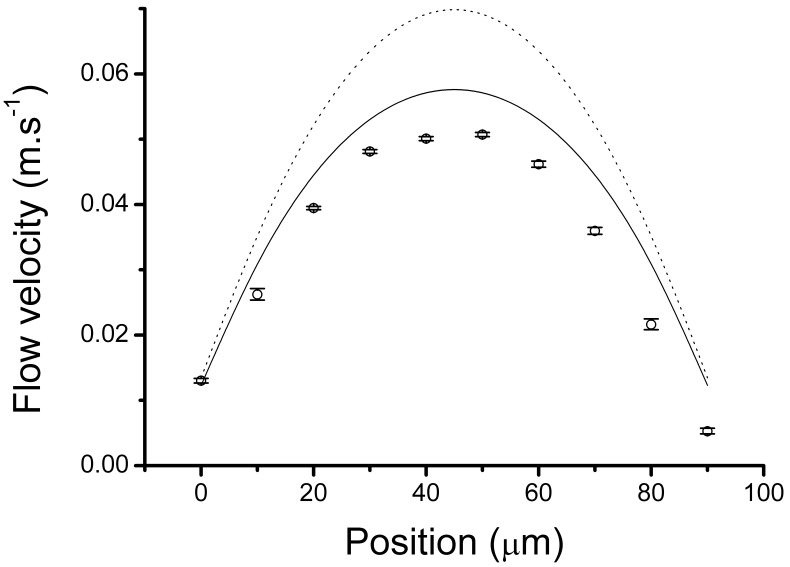

Figure 2-3. The flow velocity (experimental points) of Rhodamine Green through the width of the capillary shows a parabolic curve with the highest flow in the middle. Theoretical flow profiles for laminar flow in cylindrical (dotted line) and square (solid line) tubes are also presented.

The average flow velocity through the capillary is circa $3x10^{-2}$ m.s^{-1}. The difference between both values can be attributed to the parabolic flow-rate profile as shown in Figure 2-3: the highest flow velocity is in the middle of the capillary. Near the wall the flow is very slow. This parabolic flow profile is typical for laminar pressure-driven flow in tubes and has been observed already by Poiseuille in the 18th century (Sutera, 1993). Similar results were reported by Gösch *et al.*, (2000).

The flow profile for a cylindrical tube is given by Poiseuille's law (Resnick *et al.*, 1992):

$$\nu_x = \frac{1}{4\mu}(R^2 - x^2)\chi \qquad (2\text{-}6)$$

where ν_x is flow velocity at position x along the axis, R is radius of the tube and μ is the dynamic viscosity of the liquid.

The pressure drop per length of a cylindrical tube is given by Pozrikidis, (2001):

$$\chi = \frac{-\Phi 8\mu}{\pi R^4} \qquad (2\text{-}7)$$

where Φ is the flow rate. Using Eqs. 2-6 and 2-7 the measured flow profile deviates from this theoretical curve using $\Phi = 2.78\text{x}10^{-10}$ $m^3.s^{-1}$ (flow rate of 1 $ml.h^{-1}$), $\mu = 1.002\text{x}10^{-3}$ $kg.m^{-1}.s^{-1}$ and R= 50 µm (see Figure 2-3, dotted line).

Let us now discuss the velocity distribution in a rectangular tube for which an expression has been derived by Pozrikidis, (2001). The velocity distribution for a rectangular tube can be expressed by an infinite series:

$$v_x(y,z) = \frac{\chi + \rho g_x}{2\mu} b^2 [1 - \frac{z^2}{b^2} + 4\sum_{n=1}^{\infty} \frac{(-1)^n}{\alpha_n^3} \frac{\cosh(\alpha_n \frac{y}{b})}{\cosh(\alpha_n \frac{a}{b})} \cos(\alpha_n \frac{z}{b})] \qquad (2\text{-}8)$$

where $v_x(y,z)$ is the velocity at point x at area (y,z), $2a$ and $2b$ are the side-lengths of the rectangular tube, ρg_x is the product of density and gravity and $\alpha_n = \pi(n\text{-}½)$. For the flow rate Φ the following equation has been obtained (Pozrikidis, 2001):

$$\Phi = \frac{\chi + \rho g_x}{3\mu} 4ab^3 [1 - 6\frac{b}{a}\sum_{n=1}^{\infty} \frac{1}{\alpha_n^5} \tanh(\alpha_n \frac{a}{b})] \qquad (2\text{-}9)$$

Figure 2-3 shows the theoretical flow profile in our square capillary using $\Phi = 2.78\text{x}10^{-10}$ $m^3.s^{-1}$, $\rho g_x = 0$, $a = b = 50\text{x}10^{-6}$ m, $\mu = 1.002\text{x}10^{-3}$ $kg.m^{-1}.s^{-1}$ and z=0. Now, the theoretical curve gives a better approximation to the experimental data than the cylindrical model (see Figure 2-3, solid line).

Bacteria in a capillary

E. coli cells harbouring the fluorescent protein EYFP or EGFP were injected into the capillary. Brownian movement of the bacteria causes them to pass through the detection volume, creating photon bursts of > 10^6 photons per second (see Figure 2-4A). The photon stream was autocorrelated in real-time (see Figure 2-4B). The bacteria had a τ_{diff} in the order of several milliseconds. When the bacteria were flown through the capillary, the autocorrelation curves apparently show a much shorter diffusion time (see Figure 2-5). The photon bursts dropped dramatically to 10–75x10^3 photons per second because the residence time of the fluorescent particles in the detection volume is much shorter. Upon increasing the concentration of the bacterial cell suspension, the time between single events decreased and the amplitude of the autocorrelation trace became smaller (see Figure 2-6). The amplitude of the autocorrelation curves, *G(0),* scales inversely with the number of particles (see Eq. 2-1).

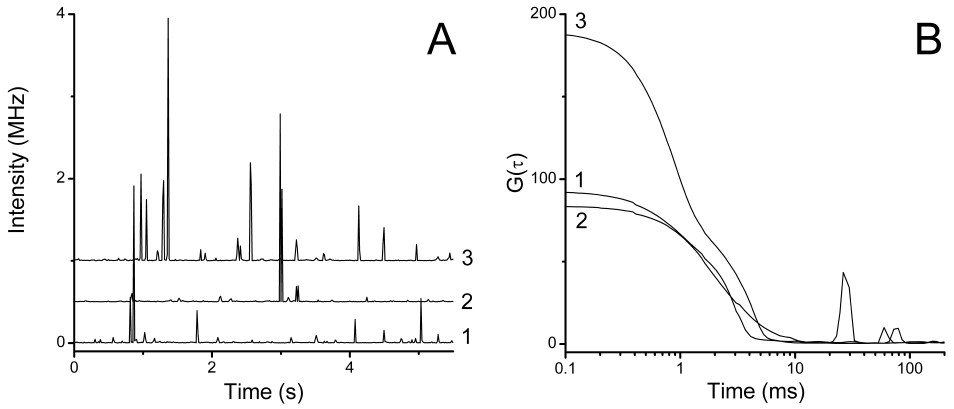

Figure 2-4. A. Photon bursts are observed when *E. coli* bacteria containing EYFP diffuse through the femtoliter detection volume. Three curves have been stacked for reasons of clarity.

B. The autocorrelation curves show a large spread in diffusion times. The three measurements were 5.5 seconds long.

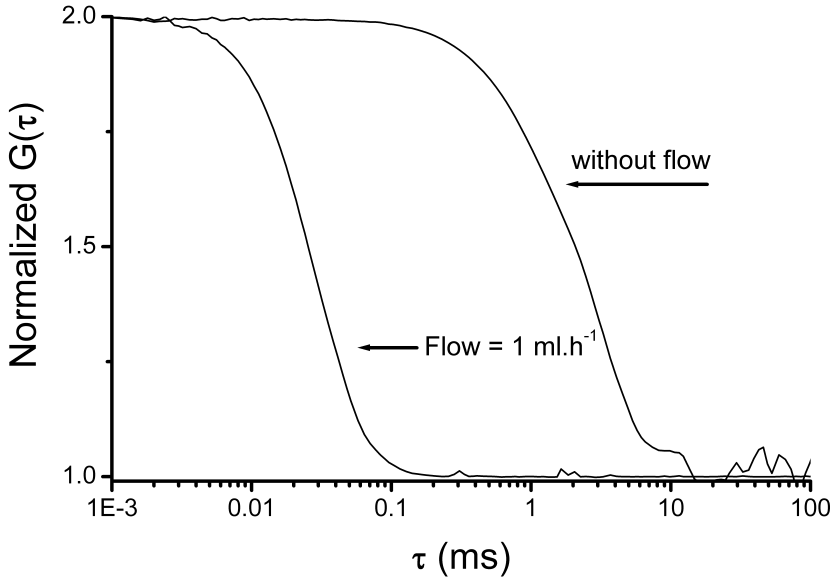

Figure 2-5. Normalized autocorrelation traces of *E. coli* bacteria containing EYFP with and without flow measured during a one-minute period.

In the absence of flow we observed that the diffusion time of a single bacterium was between 1 and 15 ms. Diffusion times depend on the followed trajectory through the confocal volume element. The volume of the CVE is similar to that of bacteria. This has implications for the applied fcs-flow model, since this model is based upon travelling of relatively small fluorescent molecules through the much larger CVE (Magde *et al.*, 1974). It can be imagined that the exact value of τ_{diff} is dependent on that part of the particle, which is transiently in the CVE. The τ_{diff} will be shorter than expected when only the tips of a bacterial cell are in the CVE. Therefore, the value of τ_{diff} is not accurately defined. For more accurate determination of τ_{diff} the CVE must be made larger.

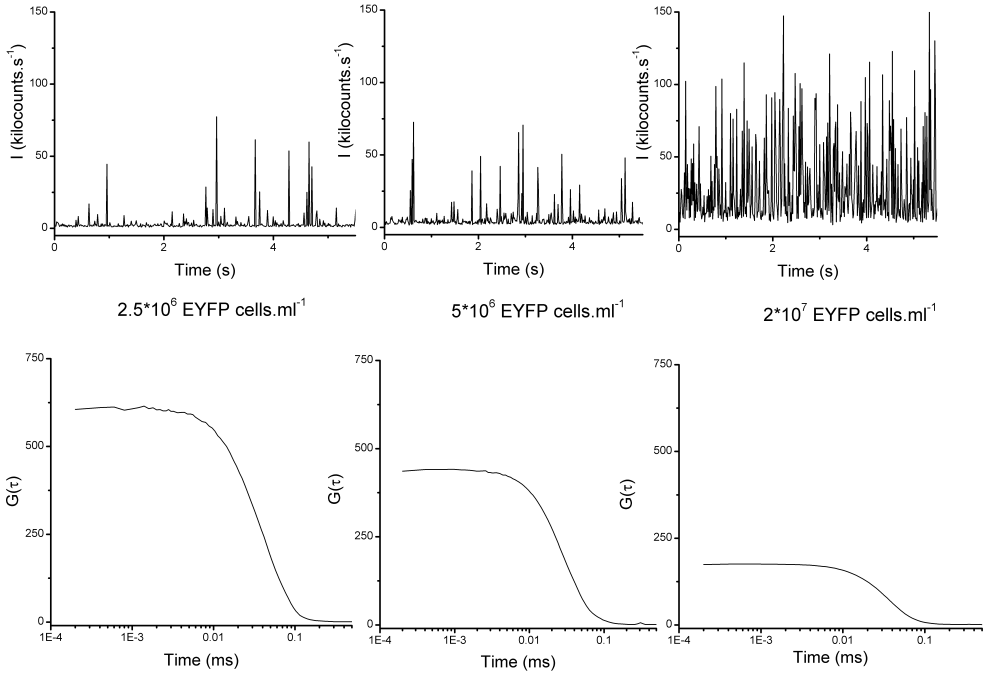

Figure 2-6. Influence of the concentration of *E. coli* bacteria containing EYFP on the fluorescence intensity traces (upper panel) and the corresponding autocorrelation curves (lower panel) at a flow rate of 1 ml.h^{-1}. The autocorrelation curves have been obtained during a one-minute period.

The flow velocity itself was calculated from τ_{flow} using Eq. 2-5. The flow velocity of bacteria is smaller than the flow velocity of relatively small molecules like EYFP protein (27 kDa) or Rhodamine Green (see Figure 2-7, in which the flow velocities obtained using the fcs-flow model versus the laser power have been summarized for all fluorescent systems studied). The pump flow was held constant at a flow rate of 1 ml.h^{-1}. Furthermore, the apparent flow velocity of bacteria depends on the laser intensity. Experiments in which mixtures of fluorescent and non-fluorescent bacteria were used showed that there is no influence of the non-fluorescent bacteria on the apparent flow velocity. Because they have a better-defined shape, the flow velocity of fluorescent microspheres of different sizes was measured to investigate the nature of the dependence on laser intensity.

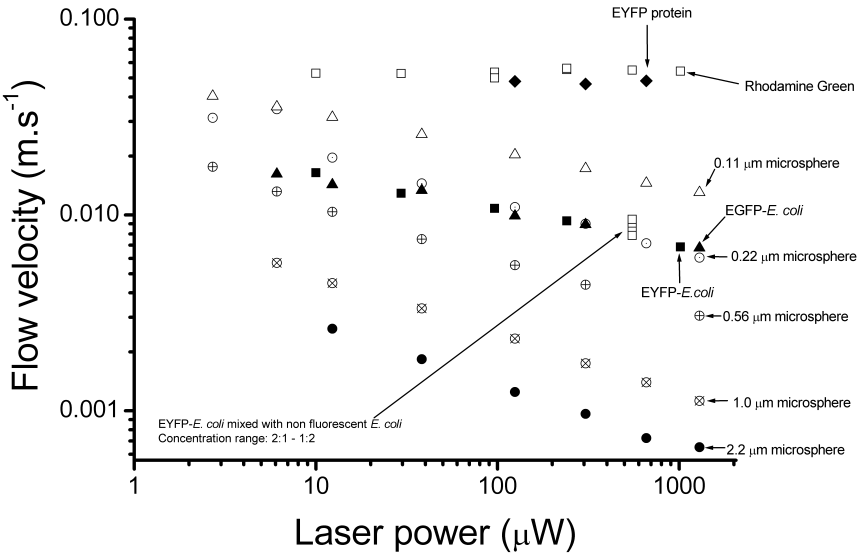

Figure 2-7. Variation of laser power does not have influence on the flow velocity of small molecules like isolated EYFP and Rhodamine Green. In contrast, the laser intensity influences the (apparent) flow velocity of macroscopic particles like bacteria and microspheres. Larger particles are more retarded than smaller particles and higher laser power leads to more retardation.

Microspheres in a capillary

Green-yellow fluorescent microspheres of sizes ranging from 0.11 μm to 2.2 μm were introduced in the capillary flow and the flow velocity was determined as described in the previous paragraph. Initially, we used a fixed value (the average of many measurements) for τ_{diff} in the analysis of flow experiments at fixed flow rates. This procedure was described for small molecules but experiments were not carried out for macroscopic particles (Gösch *et al.*, 2000). When τ_{diff} is not fixed in the fitting procedure, the fit improved considerably signified by a lower, relative χ^2 (goodness-of-fit criterion). However, no significant influence has been found on the τ_{flow} values. This is illustrated in Table 2-1, summarizing the recovered parameter values of experiments of 0.56 μm microspheres with different laser light intensities. It is also clear from the data in Table 2-1 that τ_{flow} and τ_{diff} become longer when the laser intensity increases and that there is a distinct correlation between their values.

	A					B		
Laser Power µW	τ_{flow} µs	Confidence Interval (67%)	τ_{diff} µs	Confidence Interval (67%)	χ2	τ_{flow} µs	Confidence Interval (67%)	χ2
1295	102	99.8 – 103	130	123 – 136	9.0 E-5	95.1	91.5 – 98.2	2.4E-3
306	70.9	70.8 – 71.4	85.9	83.4 – 87.8	1.4 E-4	68.6	64.6 – 72.2	9.3E-3
125	56.4	56.4 – 56.8	68.2	56.8 – 70.1	4.3 E-4	56.2	52.9 – 59.4	2.4E-2
38.2	41.5	41.5 – 41.8	52.0	50.0 – 54.0	2.0 E-3	42.3	40.0 – 44.5	6.2E-2
12.3	30.2	30.1 – 30.3	42.4	40.3 – 44.4	7.5 E-3	31.6	30.3 – 33.1	0.13
6.1	23.7	23.7 – 23.9	38.1	36.2 – 40.5	1.8 E-2	25.3	24.1 – 26.4	0.21
2.7	17.9	17.4 – 17.9	32.4	29.9 – 35.1	6.1 E-2	19.0	18.4 – 19.7	0.39

Table 2-1. The influence of τ_{diff} fixation on the τ_{flow} of microspheres using the fcs-flow model. Flowing microspheres (0.56 µm, 1 ml.h^{-1}) are investigated using different laser intensities. The autocorrelation curves are fitted to the fcs-flow model with a fixed (B) and non-fixed (A) τ_{diff} parameter. Microspheres have diffusion times in the range of several milliseconds. Fixation of τ_{diff} to 2.5 ms has no profound effect on the obtained τ_{flow} values, but on the goodness of fit signified by a higher relative χ^2. Confidence intervals were obtained after an exhaustive search as described by Beechem *et al.* (1991).

The physical meaning of the apparently anomalous τ_{flow} and τ_{diff} will be addressed in the next paragraph. The laser intensity has the same effect as observed in the experiments with fluorescent bacteria: The higher the laser intensity, the slower the microspheres appeared to flow (Figure 2-7). Furthermore, larger microspheres are flowing slower than smaller ones. The relatively small EYFP protein and the calibration dye, Rhodamine Green, have the same flow velocity that is independent of the applied laser intensity. The rod-shaped *E. coli* bacteria flow with a similar apparent velocity as spheres of 0.22 µm.

Similarly as shown for Rhodamine Green (Figure 2-2) the apparent flow velocities of microspheres of 0.22 µm and 0.56 µm size scale linearly with the pump settings (results not shown).

Further evidence for retardation of particles during detection came from direct observations of the photon pulses of flowing fluorescent microspheres using a digital storage oscilloscope (flow rate: 1 ml.h^{-1}, 2x10^6 0.56 µm microspheres.ml^{-1}, 125 µW 488 nm laser power). An individual photon burst typically consists of 100-150 photon pulses (counts) and a single burst lasts on average approximately 50-60 µs. This number is comparable to the results from fcs-flow analysis of flowing microspheres (see τ_{flow} in Table 2-1). These photon bursts therefore represent the passage of one fluorescent particle. The

duration of the burst is almost five times larger than the 13 μs residence time of a flowing Rhodamine Green molecule. In other words, microspheres are retarded in their flow during passage through the CVE.

With the FCS instrument the photons are counted and stored in so-called bins. The minimum bin time was determined by the electronics and was 13.5 ms. In the 13.5 ms bins we observed, for example, bursts as high as 10^6 photons per second, when fluorescent bacteria passively diffused through the CVE. When they were flown through the capillary with a flow velocity of $5x10^{-2}$ $m.s^{-1}$, photon bursts of $5x10^4$ photons per second were observed corresponding to circa 675 photons counted per bin. These numbers are based on the average of many particles and are not representative of the photon burst emitted by a single, passing particle. However, we can estimate the number of passing particles per unit time through the CVE. The top right panel of Figure 2-6 shows the measured photon intensity of passing fluorescent bacteria through the CVE. The averaged photon intensity was calculated to be $27x10^3$ photons per second (corrected for background). When we assume that one particle emits 100 photons then on average 3.6 particles is counted in one bin. This corresponds to approximately 270 particles per second.

Optical forces on microspheres

The obtained flow velocity using large fluorescent particles like bacteria and microspheres is smaller than the flow velocity of calibration dyes. To investigate this further, the behaviour of microspheres was observed using different laser light intensities. Several 2.2 μm microspheres in a 96-well plate with a flat borosilicate bottom could be viewed through the ocular eyepiece of the ConfoCor I setup. The microspheres could be trapped with a laser power of around 1 mW using a wavelength of 488 nm. A captured microsphere was seen as a fluorescent particle around the focal point of the laser beam and it did not move when the wells plate was slowly moved using the translation stage of the microscope (non-trapped particles did move). The trap could easily loose the particle by a fast movement of the well plate. It was not possible to visibly trap smaller particles or using less laser power. In other words, the influence due to radiation pressure on dielectric particles of μm size like microspheres is weak but present and plays a role in the retardation of flowing particles. The flow retardation is related to optical laser trapping (Ashkin, 1970, 1992, 1997; Svoboda and Block, 1994; Wright *et al.*, 1994) since that phenomenon depends on the laser intensity and particle size. Now the correlation between τ_{flow} and τ_{diff}

as function of the laser intensity becomes clear (see Table 2-1). When the flow is retarded, the diffusion must be equally affected, since free diffusion does not take place any more.

Let us now try to estimate the forces that act on these particles. Optical forces are usually defined by the following relationship (Ashkin, 1992; Svoboda and Block, 1994; Wright *et al.*, 1994):

$$F_{trap} = \frac{Q\eta P}{c} \qquad (2\text{-}10)$$

where Q is a dimensionless efficiency parameter, η is the refractive index of the surrounding medium, c is the speed of light *in vacuo* and P is the incident laser power. The efficiency parameter Q represents the fraction of the power used to exert force. It takes into account the convergence angle, spot size, wavelength, polarization and point spread function of the incident light. Q also contains parameters related to the optical properties of the trapped particle like size, shape and refractive index. The maximum force that can be created is when $Q = 1$. When the laser power is 1 mW, the maximum force is equal to circa 4.4 pN.

The drag force is given by Stokes law (Wright *et al.*, 1994):

$$\Delta F_{drag} = -6\pi\mu\Delta v r \qquad (2\text{-}11)$$

where μ = dynamic viscosity, r = radius of sphere and Δv = difference between initial flow velocity and measured flow velocity during passage through the CVE. When we use the Stokes equation to obtain the drag force for 0.56 μm spheres using Δv ($\Delta v \approx 0.047$ m.s^{-1}, see Figure 2-7), drag forces are between 300 and 400 pN. These numbers are clearly too high. We can draw two conclusions from these results. Optical trapping theory for particles in a flow has to be critically examined. For cases where the particles are of similar size as the CVE, FCS experiments have to be repeated for an optical geometry in which the CVE is much larger than the particle size.

Conclusions

We have used FCS to detect flowing fluorescent particles and molecules in a capillary. With these experiments the basic prerequisites for confocal detection of fluorescent particles in complex microfluidic biochips have been fulfilled. In these biochips detection and sorting of biolibraries

takes place within milliseconds. The parameters for successful detection have been elucidated. For example, the temporal detection window of a flowing fluorescent particle depends on the bulk flow rate and can be as low as 50-100 μs. In this time window a photon burst of approximately 100 photons can successfully be distinguished from the ubiquitous background.

The flow velocity can be determined from a fcs-flow model. For large particles (> 0.2 μm) the recovered flow velocities are dependent on the laser intensity and their radius. These particles seem to be retarded in the confocal detection volume due to optical forces. The real nature of this retardation by laser illumination requires further investigation.

When using a microfluidic biochip setup for screening of particle-based bio-libraries one should take into account that the time needed to detect particles with highly focused laser light cannot be easily determined from the flow velocity of the liquid. This time should be found empirically.

Acknowledgements

This research has been supported by the Technology Foundation STW, the applied science division of The Netherlands Organization for Scientific Research NWO and the technology program of the Ministry of Economic Affairs (grant WBI 4797). We thank Jan Willem Borst for making available fluorescent proteins and fluorescent bacteria. We appreciate stimulating discussions with Marileen Dogterom, Mark Hink, Robin M. Schoemaker and Jan Rinze Peterzon.

Chapter 3

Towards sorting of biolibraries using single molecule fluorescence detection techniques

The selection of specific binding molecules like peptides and proteins from biolibraries using, for instance, phage display methods can be quite time-consuming. It is therefore desirable to develop a strategy that is much faster in selection and sorting of potential binders out of a biolibrary. In this contribution we separately discuss the current achievements in generation of biolibraries, single-molecule detection techniques and microfluidic devices. A high-throughput microfluidic platform is then proposed that combines the propulsion of liquid containing fluorescent components of the biolibrary through microchannels, single-molecule fluorescence photon burst detection and real-time sorting of positive hits.

This chapter has been published as:

A.J.W.G. Visser, B.H. Kunst, H. Keller and A. Schots
C*urrent Pharmaceutical Biotechnology,* 2004*,* **5***,* 173-179.

Reprinted with permission of the Bentham Science Publishers Ltd.

Introduction

The general motto of this chapter is "the way down from single genes, and proteins to single molecules". Where to start? Either from the top down beginning with medicine or from the bottom up beginning with single molecules and their behaviour? The answer is a typical compromise: working in both directions from the middle. We can extrapolate this way of thinking a little further and more generally to the field of imaging of cellular systems, even when we have constrained our topic by focusing on biolibraries as a biological system and single-molecule fluorescence detection as a helpful tool for sorting and selection. There is a transition occurring in biology from the molecular level to the system level that promises to revolutionize our understanding of complex biological systems (Kitano, 2002). Understanding of genes and proteins remains centrally important and forms the basis of understanding the organization and dynamics of a biological system. Techniques and methods developed within the field of genomics and proteomics ranging from sequencing to yeast two/three hybrid methods, mass spectrometry and DNA/protein arrays, continue to be important and even need further development. However, breakthroughs in experimental devices, advanced software and analytical methods allowing *in vivo* imaging are required before the achievements of 'systems biology' can live up to their much heralded potential (Kitano, 2002). Only then will we be able to examine the structure and dynamics of cellular and organismal function. This will, in turn, lead to an understanding of the mechanisms that systematically control the state of the cell and multicellular structures. System-level insight will then allow the modification and (re)construction of biological systems having desired properties using genetic methods or by using mechanism-based drugs (Kitano, 2002). Therefore, understanding the properties of biomolecular networks is of central importance in basic biological science and in biomedicine of importance to human health. Modern microspectroscopic techniques (that can be considered as a combination of microscopic and spectroscopic techniques) are the method of choice for the above purpose as these techniques provide direct information on molecular interactions and dynamic events involving biomolecules with minimal perturbation of cellular integrity and function. Thus, the wealth of information and resources generated by efforts in genomics and proteomics can be directly translated into understanding the functioning of cells, tissues and organisms *in vivo*.

The further development of modern microspectroscopic techniques is also relevant for the subject that we want to emphasize here: biolibraries,

how can we screen and sort them, and with which techniques? The same microspectroscopic techniques (single-molecule fluorescence detection in particular) can be used for screening and sorting of biolibraries as for optimizing cellular imaging systems. In both cases it is important to develop optimum contrast schemes between the reporting fluorescence signals and the background signals (actually eliminating background signals arising from Raman and Rayleigh scattering and spurious fluorescence) resulting in the highest level of sensitivity, precision and speed of measurements, temporal and spatial resolution. We will also need microfluidic systems for the downscaling of sorting and selection of biolibraries. These microfluidic devices also require techniques to control passage of the fluid as well as to determine the flow speed in minute volumina. Considering all possible microspectroscopic parameters fluorescence analysis of biolibrary components is particularly attractive, as its sensitivity is high enough to detect single molecules in aqueous solutions and its detection time short enough to enable on-the-fly measurements.

This minireview has been divided into the following topics: (i) biolibraries, (ii) single-molecule fluorescence techniques, (iii) microfluidic devices, (iv) possible ways of integrating topics i-iii into a working prototype.

Biolibraries

The organization and dynamics of biological systems rely on an intimate interplay of (macro-)molecules. Proteins, nucleic acids and other compounds interact with each other to transduce signals or to build up macromolecular structures that shape cells and organelles. Cell functioning largely depend on protein interaction networks or as outlined by Alberts (1998) ‘the entire cell can be viewed as a factory that contains an elaborate network of interlocking assembly lines, each of which is composed of a set of large protein machines’. Unravelling protein interaction patterns is therefore of key importance to increase our understanding of cell function. Efforts in the fields of genomics and proteomics have increased our knowledge in this field considerably. It remains, however, required to use techniques to identify interacting partners using the appropriate techniques. Peptide and cDNA libraries have shown to be of great significance for this purpose when used in combination with techniques to find interactors such as yeast two/three hybrid systems, phage display and protein and DNA arrays.

Recent developments in microspectroscopy as well as new expression and labelling strategies enable a more specific and sensitive selection of peptides and proteins from peptide and cDNA libraries expressed on phage or bound to

a solid surface as, for instance, used with arrays. Regarding the latter it has now been shown that overexpression of cDNAs in expression vectors using cell microarrays can be used to identify genes in diverse cellular processes (Wu *et al.*, 2002). A glass slide is printed with cDNA in an aqueous gelatine solution. The slides are then incubated with mammalian cells and transfected using a lipid transfection agent. Clusters of ~30-80 cells actively express the (defined) gene products that can be visualized using a variety of microspectroscopic techniques.

Regarding the expression of cDNA libraries on bacteriophage one can use filamentous and lytic phages. Filamentous phages such as M13, fd and IKE infect *E. coli* bacteria through their gene III protein (gIIIp) that binds to pili. Upon replication of the phage genome new phages are assembled and excreted from the bacteria without cell lysis. All five proteins present in the phage coat have been used for display. However, for cDNA phage display the gIIIp and gVIp proteins are most important, using gIIIp for expressing N-terminal and gVIp for C-terminal fusion proteins. Instead of filamentous phage an increasing use is being made of lytic phages such as phage λ and T7. These phages infect the bacterial cell and replication and assembly is followed by a real phage burst resulting in cell lysis. The protein forming the 'head' of the phage is used for display. The choice of the display system for cDNAs depends on the goals to be achieved as well as personal preferences and experiences. Jespers *et al.* (1995) were the first to use cDNA phage display. They displayed a cDNA library from the hookworm *Ancylostoma caninum* on the gVIp of M13 and found two genes encoding novel members of two different families of serine protease inhibitors. Many applications of cDNA phage display have followed since, including the isolation of lectins (Yamamoto *et al.*, 1999), lysosomal proteins (Shanmugavelu *et al.*, 2000), SH2 proteins (Cochrane *et al.*, 2000), allergens (Eriksson *et al.*, 2001; Kleber Janke *et al.*, 2001; Weichel *et al.*, 2003), antigens (Sioud *et al.*, 2000), proteins involved in various signalling pathways (Bianco *et al.*, 2002; Zhou *et al.*, 2003) and many more.

Not only cDNA libraries but also peptide libraries are important in elucidating protein interaction networks and signalling pathways (for a review see Turk and Cantley (2003)). Peptide library approaches can be broadly grouped into methods employing either synthetic or encoded libraries. Synthetic libraries are bound to a solid support such as beads or microarrays. In many screening strategies fluorescent receptor proteins are being used. Encoded libraries are usually displayed in bacteriophages.

In most of the studies applying phage display, panning procedures or variations thereof have been used for selecting genes encoding interacting

proteins. Several rounds of selection are usually required to end up with a number of phage clones one can handle for characterization. This may result in a loss of rarely expressed genes and of genes encoding proteins having a lower affinity for the bait protein. The latter may be a consequence of a truncated or partial cDNAs in the library. Interesting genes may thus be lost. Microspectroscopical methods facilitate the development of new selection strategies based on single-molecule detection and whole-cell imaging resulting in an integrated approach as outlined in the final paragraph.

Single-molecule fluorescence detection techniques

Fluorescence parameters of biomolecules are the quantum yield (Q) (or the fluorescence intensity), the lifetime of the excited state (τ), the radiative lifetime (τ_r), the emission and excitation (absorption) spectra, and the anisotropy (Lakowicz, 1999). All these parameters can be determined in bulk measurements using conventional fluorescence instruments that are mostly commercially available. In contrast, there is also a wealth of information available from single-molecule fluorescence measurements that resulted in novel applications notably in analytical chemistry, pharmaceutical sciences and biotechnology. Here we will highlight Fluorescence Correlation Spectroscopy (FCS) and, in general, single-molecule fluorescence detection techniques, as these techniques can be used to detect sparse, fluorescent molecules in a flow and to measure flow velocities of these molecules.

FCS was introduced in the 1970s as a method for measuring molecular diffusion, reaction kinetics and flow of fluorescent particles (Elson and Magde, 1974; Magde *et al.*, 1972, 1974). The underlying principles of FCS laid the foundation for a whole series of methods that are collectively referred to as fluorescence fluctuation spectroscopy. In the early 1990s we could observe a renewed interest in FCS owing to considerable progress in instrumentation (stable lasers, confocal excitation and detection, avalanche photodiodes, high-speed correlators, faster computers, etc.) (Rigler *et al.*, 1993), offering novel applications in biotechnology (Eigen and Rigler, 1994; Rigler, 1995).

FCS measurements can be carried out in an optical, confocal microscope. In FCS small spontaneous deviations from thermal equilibrium in an open system are reflected by fluctuations in the fluorescence intensity induced, for instance, by fluorescent molecules diffusing into and out of a well-defined observation volume generated by a focused laser beam. The laser beam continuously illuminates a fixed region within the sample. Although fluorescent particles throughout the excitation volume are excited, only the fluorescence

from particles is detected through a pinhole positioned at the image plane of the excitation volume. The observation volume is smaller than the excitation volume and, depending on the size of the pinhole and the magnification of the objective, amounts to less than one femtoliter. The observation volume has an ellipsoidal shape with the long axis being ca. 3-10 times longer than the short axis (this ratio of length and radius of the observation volume is called the structural parameter). The detector is either an avalanche photodiode or a sensitive photomultiplier operating in single-photon counting mode. Generally a pinhole is not required when 2-photon near-infrared excitation is used. The simultaneous absorption of two low-energy photons leads to an excited state and fluorescence only in the very focus of the laser beam. The excitation and observation volumes are then the same and more spherical in shape.

Each time a fluorescent molecule enters the observation volume a burst of fluorescence photons is detected. When diffusion is the only dynamic process causing intensity fluctuations, the duration of this photon burst reflects the time a particle needs to diffuse across the observation volume. Autocorrelation of the intensity trace results in an autocorrelation curve which can be analyzed to yield the average number of particles in the observation volume and the average diffusion time. The diffusion time τ_{dif} describes the dwell time of a particle in the observation volume, which is related to the diffusion coefficient D_{tran} via $\tau_{dif} = \omega_{xy}^2/(4D_{tran})$, ω_{xy} is the distance from the centre of the observation volume in the x,y plane at which the detected fluorescence intensity has decreased by a factor e^2. The amplitude of the correlation function, $G(0)$, represents the average number of molecules N found in the observation volume: $G(0) - 1 = 1/N$.

Alternatively, the amplitude of the emission bursts contains information about the molecular brightness of the particle, since bright particles will on average give rise to larger fluorescence bursts than dimmer ones. Let us consider a living cell expressing a receptor-protein construct with GFP in the plasma membrane. The receptor can form dimers in equilibrium with receptor monomers. The dimer containing two GFP molecules will emit twice the intensity as a monomeric receptor. The frequency of fluorescence intensities can be plotted against the time-binned fluorescence intensities. This is known as photon-counting histogram (PCH) analysis (Chen *et al.*, 1999) or fluorescence-intensity distribution analysis (FIDA) (Kask *et al.*, 1999). These concepts have essentially the same meaning and were developed simultaneously and independently. Analysis of this PCH yields the molecular brightness and the number of the particles. The molecular brightness can be defined as the number of detected fluorescence photons per molecule per second.

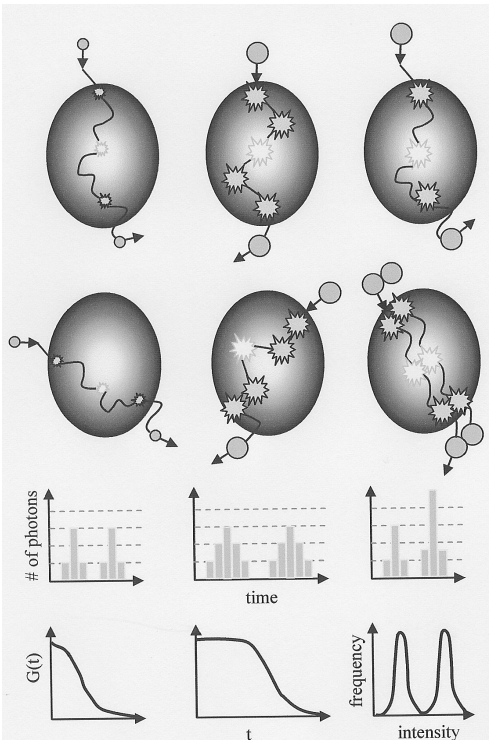

Figure 3-1. Schematic view of photon burst detection and analysis of single fluorescent molecules in a focused laser beam.
Left column: A small fluorescent molecule is entering a laser beam depicted as a prolate ellipsoid. Since the laser intensity has a Gaussian distribution, the initial intensity at the position where the molecule enters is smaller than when the molecule has traversed to the center with maximum intensity. Very soon the small molecule diffuses out of the excitation volume terminating the photon burst. A short time later another molecule enters and the process is repeated. Two Gaussian shaped intensity bursts of photons are visible in time. Many events lead to continuous intensity fluctuations, which can be autocorrelated in real time. The decay time of this trace, $G(\tau)$, represents the residence time of the molecule in the excitation volume, while the amplitude is proportional to the reciprocal number of molecules. *Middle column*: A much larger fluorescent protein molecule gives rise to longer lasting bursts and longer residence times. *Right column*: The successive photon events are registered from a single protein and two proteins forming a dimer and generating twice the number of photons. Now it is more advantageous to analyze the intensity distribution of the photon bursts. In the example the number of protein monomers is the same as that of protein dimers.

In case of the presence of dimeric receptor species in equilibrium with monomeric ones one should observe a PCH of two species and their relative concentrations. Figure 3-1 gives a pictorial view of the time- and amplitude-dependence of photon burst detection of single molecules in a focused laser beam. Besides measurements of local concentrations, diffusion times and brightness values, fluorescence fluctuation spectroscopy is capable of observing a whole range of other dynamic processes that give rise to fluctuations in the fluorescence signal. Comprehensive reviews (Bacia and Schwille, 2003; Hess *et al.*, 2002; Thompson, 1991) and a book (Rigler and Elson, 2001) dedicated to this technique clearly demonstrate its versatility.

Because of its small, confined detection volume and its large sensitivity FCS is especially suitable for measurements in microfluidic devices. It is therefore not surprising to see that FCS have been used to determine flow profiles and flow speeds of fluorescent molecules and particles in

microcapillaries or microstructured channels (Gösch *et al.*, 2000; Kunst *et al.*, 2002; Lenne *et al.*, 2002). The theoretical framework for FCS analysis of transport by flow, superimposed on transport by diffusion, has been given in (Magde *et al.*, 1978). When there is active transport in the form of laminar flow, the autocorrelation function $G(\tau)$ also contains a 'flow' component with a characteristic time τ_{flow}, that is the average flow time of the fluorescent particles through the detection volume (Brinkmeier *et al.*, 1999; Gösch *et al.*, 2000). The flow velocity v is given by $v = \omega_{xy} / \tau_{flow}$.

The minimum flow velocity that can be measured is determined by Brownian diffusion. When the flow velocity is too small, it becomes difficult to distinguish between diffusion alone and diffusion superimposed on flow. Therefore, τ_{flow} must be distinctly shorter than the diffusion time, τ_{dif}, in order to recover the flow velocity from the analysis. In our facilities at Wageningen University the recorded autocorrelation curves are analyzed using in-house developed global analysis software enabling the determination of parameters τ_{dif} and τ_{flow} see Kunst *et al.* (2002) for details. In Figure 2-5 we have presented examples of autocorrelation traces of flowing *E. coli* bacteria expressing Yellow Fluorescent Protein (YFP).

Although analysis of FCS curves allows accurate determination of flow velocities, the flow direction of particles being transported through the observation volume cannot be established exactly. A few groups have circumvented this problem by employing two focused laser beams that are spatially separated by a defined distance and by cross-correlating the respective emission signals (Brinkmeier *et al.*, 1999; Dittrich and Schwille, 2002). In case of directed flow, each single fluorophore successively passes the two focused beams aligned in the direction of the flow and resulting in a cross-correlation curve with a distinct maximum that corresponds to the transition time between the volumes.

Of course, one can determine the flow rate of fluorescent particles in a continuous liquid flow very accurately from FCS analysis (see Figure 2-5). However, if one wants to use flowing, fluorescent particles for sorting and deflection in a microfluidic device, there is simply no time for generating a good signal-to-noise FCS-curve (note that the autocorrelation traces in Figure 2-5 were measured during one minute). Therefore, one should simply capture the burst of emission photons when fluorescent molecules transit a focused laser beam. Since almost two decades large progress has been made in the detection of single fluorescent molecules in liquids at ambient temperature (Keller's group in the USA has made pioneering efforts as reviewed in detail in (Ambrose *et al.*, 1999)). Let us first estimate the number of photons that can be

detected from a single fluorescent molecule that transits a laser beam tuned to an optical transition. During the transit time in the beam the molecule undergoes cycles of photon absorption and emission giving off a photon on most cycles. The maximum number of photons emitted in a burst is approximately equal to the transit time divided by the fluorescence lifetime. For a transit time of 1 ms and a lifetime of 1 ns this maximum number is 10^6. In practice, however, photodecomposition limits this number to ~10^5 photons even for very stable molecules. The detection efficiency of the optical microscopic systems used in single-molecule studies amounts to ~1%. Therefore we expect a burst of ~1000 photons when a single, strongly fluorescent molecule crosses the laser beam. An example of a photon burst emitted by *E. coli* bacteria (containing many YFP copies) flown through a micro-capillary is given in Figure 2-6 (upper panel). In this example the minimum bin time in which the photons are counted and stored is 13.5 ms (this time is limited by the electronics of the commercial instrument). In this relatively long bin time bursts as high as 10^6 photons/s can be observed. When the bacteria were flown through the capillary with a velocity of $5x10^{-2}$ $m.s^{-1}$, photon bursts of $5x10^4$ $photons.s^{-1}$ were observed corresponding to ~675 photons counted per bin. This number is based on the average of many particles and is not representative for the photon burst of a single particle. We can estimate the number of passing particles through the laser beam from Figure 2-6 (upper right panel). The average photon intensity was ~$27x10^3$ $photons.s^{-1}$. When we assume that one particle emits 100 photons, ~270 $particles.s^{-1}$ are passing through the laser beam, corresponding to ~3.6 particles counted in one bin.

Several other groups have reported on detection of single molecules in microstructures (Dörre *et al.*, 2001; Lee *et al.*, 1994; Lyon and Nie, 1997; Mathis *et al.*, 1997; Nie *et al.*, 1995; Nie and Zare, 1997; Zander *et al.*, 1998) and even in submicrometer-sized fluidic channels (Foquet *et al.*, 2002).

There is considerable interest in using microfabricated fluidic devices as a tool for microflow cytometry (or micro-fluorescence activated cell sorter, μFACS). The particles are transported electrophoretically by applying potentials to the fluid reservoirs. For interrogation of the fluorescent particles use is made of on-the-fly detection of fluorescence photon bursts. After burst detection the particles are deflected in another channel by changes in the applied high-voltage settings. The groups of Quake and Ramsay have made important contributions in this field (Fu *et al.*, 2002; Fu *et al.*, 1999; McClain *et al.*, 2001). Fluorescent bacteria could be separated from a background of non-fluorescent bacteria. Further details are given in the next section.

Microfluidic devices

In the last couple of years microfabricated devices have shown a plethora of novel bioanalytical applications such as macromolecular separation, biomolecular sensing and biochemical assays. They all have in common the downscaling of various (bio)chemical processes, which comprise reaction kinetics, separation of reaction products, detection of biomolecules (sensing) and applications involving cells (cellomics). Microfluidic devices are composed of micrometer channels and microliter reservoirs that are capable of transferring and storing tiny amounts of liquids in volumes of nano- and picoliters. Integrated microfluidic systems combine channels of microscopic geometry with miniaturized pumps, mixers, valves, electric components and light detectors. Such integrated systems are known as Micro Total Analysis Systems (μTAS) or 'lab-on-a-chip' systems in which it is in principle possible to automate a complete analytical process sequentially from sample preparation, reaction, to separation and detection. Many aspects of μTAS are highlighted in recent literature. Fundamental technical issues still need to be solved before the devices can be industrialized (Mitchell, 2001). The fluid behaviour in microchannels is completely determined by diffusion making equilibrium mixing (quadratically) faster with smaller sized channels (Meldrum and Holl, 2002). Considerable details of μTAS have been reviewed recently (Auroux *et al.*, 2002; Reyes *et al.*, 2002). Chovan and Guttman (2002) have summarized the application of microfabricated devices in biotechnology and bioprocess engineering. Recently, Andersson and van den Berg (2003) have published a comprehensive review on the use of microfluidic devices for manipulation of single cells (sampling, trapping, sorting, lysis, poration, fusion: in short cellomics).

Miniaturization offers various advantages over macro-scale laboratory operation: (i) reduced sample volume and less reagents thereby reducing the costs of reagents, (ii) faster reactions and reagent mixing are possible, (iii) superior heat and mass transfer eliminating thermal side-effects, (iv) more accurate measurements, (v) low-cost compact system design in which more functionalities can be integrated or operated in parallel, (vi) as a result of (v) it is foreseen that microfluidics technology can be mass-produced, (vii) development of miniaturized high throughput screening systems (Auer, 2001; Wölke and Ullmann, 2001).

Much progress has been made in the development of materials needed to make microfluidic devices and the various ways to direct liquid flow inside

microchannels. Soft lithography using elastomeric materials has been shown to be an alternative to standard photolithographic and wet chemical etching including the fabrication of valves and pumps (Quake and Scherer, 2000; Unger *et al.*, 2000). The fluid is usually driven by pressure or vacuum or by electrical means (electro-osmotic flow or electrophoresis). The direction of fluid flow can be diverted by various methods such as mechanical valves or by changing voltage gradients. Flow control can be performed by using microfluidic valves of hydrogels in microfluidic channels in glass substrates that open or close depending on the pH of the solution (Beebe *et al.*, 2000). The latter research group has been experimenting with surface-directed flow that allows aqueous liquids to be confined to hydrophilic pathways flanked by hydrophobic 'walls' inside microchannels (Zhao *et al.*, 2001). With the advantage of having no moving parts such as pumps and valves, electrocapillary pressure as a technique to drive the flow along microchannels has been developed (Prins *et al.*, 2001). When working with cells glass microchannels have been coated with poly(dimethylacrylamide) to minimize cell adsorption (McClain *et al.*, 2001). Although electro-osmotic flow was inhibited in the latter case, the negative charge of the cells still allowed electrophoretic transport. Nanofluidic (instead of microfluidic) devices will be realized in the very near future owing to improvement in fabrication processes and advances in nanoscale sensing and actuation (Craighead, 2000; Quake and Scherer, 2000).

In addition to microfabricated cell sorting devices described above (Fu *et al.*, 2002; Fu *et al.*, 1999; McClain *et al.*, 2001), some other microtools for handling cells have been developed. Confinement of cells is based on dielectrophoresis that refers to the force on induced polarization or dipole charges in nonuniform electric fields (Pohl, 1978). Dielectrophoretic sorting of particles and cells has been performed in a system that operates in three stages: a beam-narrowing device for funnelling and aligning the flow, a field cage to trap cells and a switch to direct particles in an output channel (Fiedler *et al.*, 1998). This 3-D microelectrode system for funnelling, aligning, caging, switching has been further improved (Müller *et al.*, 1999). A microfabricated dynamic multi-trap array cytometer for use in parallel single-cell assays has been recently described (Voldman *et al.*, 2002). When cells are introduced into the array of traps, it turned out possible to sort cells upon the basis of fluorescent dynamic (functional) responses to stimuli.

Future developments: an integrated approach

The described developments in the fields of cell and molecular biology (biolibraries), (bio)physics (single-molecule fluorescence detection) and nanotechnology (microfluidic devices) can be integrated. This will lead to detection systems with an, as yet, unsurpassable sensitivity. Larocca and co-workers (2001) have, for instance, developed an approach wherein bacteriophages are genetically modified to transfect mammalian cells. In this approach one uses genetic fusions between (characterized) cDNAs and fluorescent proteins that are expressed in the cell and can even targeted to subcellular compartments. By combining this with appropriate imaging technologies and analysis software one can in a high-throughput fashion obtain direct information on gene expression patterns and use that information for cell sorting.

Another possibility comes from single-molecule fluorescence detection technologies. These offer new possibilities for the selection of phage displayed peptide and cDNA libraries. Upon binding of the phage to fluorescent bait on a larger particle the diffusion time will considerably increase and the burst of photons will last longer when the fluorescent particle transits the focused laser beam. Thus, photon-burst detection methods can be developed for instance in combination with micro- or nanofluidics devices. For library versus library screening one can use phages that are labelled with two different fluorescent labels and detection of coincidence photon bursts (Brinkmeier *et al.*, 1999; Li *et al.*, 2003). As demonstrated by Li *et al.* (2003) this method allows the detection of 50-100 fM of dual-labelled DNA in the presence of a 1000-fold excess of DNA labelled with a single fluorophor. We have recently developed a prototype microfluidic platform that allows sorting one- or two-coloured fluorescent particles.

Screening cell arrays (Wu *et al.*, 2002) can already be accomplished using various imaging approaches. The speed can possibly be improved by developing better steering electronics and light collection optics. However, developing appropriate control and on-line analysis software is of equal importance in this field to speed up the processing of data that come to thousands of genes expressed in this way.

Taken together, important developments are foreseen for a more rapid and reliable screening and sorting of biolibraries. This is necessary in this era of post-genomics where a rapid translation of gene sequences into gene and even cell function is of increasing importance. This not only allows us to rapidly process the wealth of information coming from the numerous genome-

sequencing efforts, both those undertaken and under way, but also helps us to acquire insight in the functioning of protein machines and, as a consequence, cells.

Acknowledgements

We gratefully acknowledge financial support from grants of the Technology Foundation in The Netherlands (STW, WBI4797) and the European Union (QLG2-CT-2001-01428).

Chapter 4

Design of a confocal microfluidic particle sorter using fluorescent photon burst detection

An instrumental system is described for detecting and sorting single fluorescent particles such as microspheres, bacteria, viruses, or even smaller macromolecules in a flowing liquid. The system consists of microfluidic chips (biochips), computer controlled high voltage power supplies, and a fluorescence microscope with confocal optics. The confocal observation volume and detection electro-optics allow measurements of single flowing fluorescent particles. The output of the avalanche photodiode (single photon detector) is coupled to a real-time photon-burst detection device, which output can address the control of high voltage power supplies for sorting purposes. Liquid propulsion systems like electro-osmotic flow and plain electric fields to direct the particles through the observation volume have been tested and evaluated. The detection and real-time sorting of fluorescent microspheres are demonstrated. Applications of these biochips for screening of bacteriophages-type biolibraries are briefly discussed.

This chapter has been published as:

B.H. Kunst, A. Schots and A.J.W.G. Visser
Review of Scientific Instruments, 2004, **75**(9):2892-2898

Introduction

A crucial requirement for screening of cellular biolibraries is the ability to detect one single cell, analyze its characteristics in real time and sort it subsequently. A commonly used instrument for screening and sorting single fluorescent particles is the Fluorescent Activated Cell Sorter (FACS). Fluorescent cells are suspended in a stream of tiny droplets and interrogated by an optical system. The fluorescence and/or light scattering from each droplet is detected and experimental data are stored in a computer for off-line analysis. The charged droplets can be sorted in real time using electrostatic deflectors. These instruments are widely used to screen populations of relatively large cells. Smaller cells or particles like bacteria or viruses are more difficult to screen because of lower fluorescence intensity and smaller scattering power. Recently, much progress has been made using cell sorters based on microfluidic devices (Dittrich and Schwille, 2003; Fu *et al.*, 2002; Fu *et al.*, 1999) enabling the fluid-phase detection and sorting of, for instance, highly fluorescent bacteria using single-molecule detection. Single molecules have been detected by means of fluorescence in relatively large capillaries (Agronskaia *et al.*, 1999; Castro and Williams, 1997; Goodwin *et al.*, 1993), micrometer sized (Chou *et al.*, 2002; Chou *et al.*, 1999; Dittrich and Schwille, 2002; Zander *et al.*, 1998) and even sub-micrometer sized channels (Dörre *et al.*, 2001; Foquet *et al.*, 2002; Foquet *et al.*, 2004; Lyon and Nie, 1997; Sauer *et al.*, 2001).

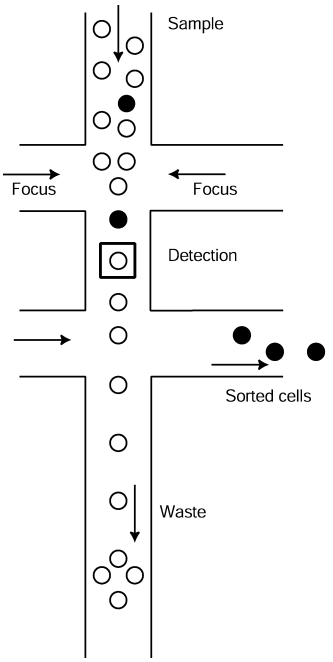

Figure 4-1. Principle of fluorescent particle sorting using microfluidic channels in a glass chip.

Previous work in our laboratories reported on the detection of flowing fluorescent particles like bacteria and microspheres in a microcapillary mounted on a confocal fluorescence microscopy setup (Kunst *et al.*, 2002). These results led to the design of a new, microfluidic biochip aimed at detection and sorting relatively small particles in real time using the same confocal fluorescence microscope. The biochip is made from glass, containing a network of channels

and reservoirs. The particles in aqueous solution are flown through the channels employing either electrokinetic forces or pressure. To increase the detection efficiency a technique (Dittrich and Schwille, 2003; Jacobson *et al.*, 2000; Jacobson and Ramsey, 1997; Knight *et al.*, 1998; McClain *et al.*, 2001; Pabit and Hagen, 2002; Pollack *et al.*, 1999; Schrum *et al.*, 1999) is used wherein two liquid inlets focus the particles into a narrow stream (see Figure 4-1). The influx of liquid into the channels was induced by either electro-osmotic flow (EOF) or electric fields in a suppressed EOF environment.

Design, fabrication and experimental set up

Design of microfluidic biochips

The biochip consists of a network of channels etched into glass (Pyrex) that are connected to reservoirs (see Figure 4-2). The channels are 45-50 μm wide and 20 μm deep and the reservoirs have a diameter of 2 mm on the top. Two lithographic masks defining the channel and reservoir structures have been designed using CleWin (WieWeb software, Hengelo, The Netherlands). The chrome masks were fabricated using a Heidelberg DWL 200 laser beam pattern generator by Delta Mask, Enschede, The Netherlands. The glass wafers were etched in buffered HF. This anisotropic etching process requires a well-designed mask, since the channel width will eventually become the design width plus twice the etched depth. Channels on the mask were designed with a width of 5 – 10 μm. Etching the channels to a depth of 20 μm resulted therefore in channels having widths of 45 –50 μm.

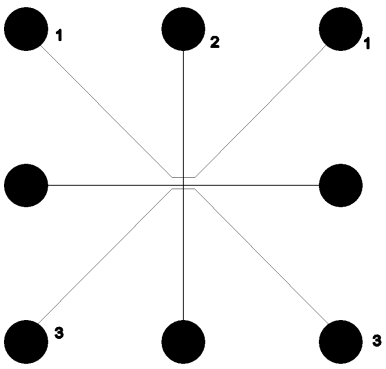

Figure 4-2. Layout of a $(12.9\ mm)^2$ square biochip. Eight reservoirs are connected to 50 μm wide and 20 μm deep channels. This particular chip design is used for experiments with emphasis on detection of single particles in combination with sorting. Reservoir 2 contains the sample, reservoirs labelled 1 are used to focus the particles into the middle of the channel and one of the reservoirs 3 is used to collect the sorted particles. The channels without numbers are not used.

Fabrication of microfluidic devices

Microfluidic devices were fabricated out of two square 4 inch glass plates, one with a thickness of 1.1 mm and the other of 175 μm, as outlined in Figure 4-3. On one side of the thick plate, a silicon layer was deposited with Plasma Enhanced Chemical Vapour Deposition. Next, a photo-resist layer was deposited and treated with a photolithography step to define the channel structure, which was subsequently transferred to the silicon layer by a reactive ion etching process. The patterned silicon layer was used as a masking layer in the etching of a 20 μm deep channel in the glass plate, using an aqueous 10 wt-% HF solution. Finally, the resist and silicon layers are stripped with acetone and with a hot aqueous 25% KOH solution, respectively.

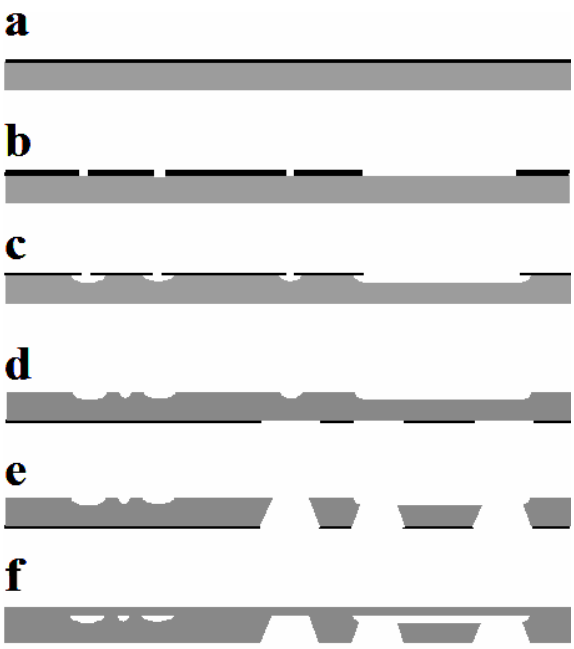

Figure 4-3. Fabrication sequence.

a) Glass plate with thin silicon layer
b) Pattern transfer from photoresist to silicon layer
c) Etching of fluidic structure in glass plate
d) Photoresist pattern on backside e) powderblasting of structure for reservoirs in backside
f) Bonding of machined glass plate to thin glass plate.

The backside of the plate was covered with a photoresist foil and treated with photolithography to define the reservoirs, which are subsequently machined in the glass by a powderblasting process, as previously described by Wensink *et al.* (2002). After removal of the resist foil and thorough cleaning of the machined glass plate, it is aligned and bonded to the thin glass plate using a thermal bonding process. Finally, the wafers were diced into individual chips.

Interfacing of microfluidic biochips

A special chip holder was constructed containing reservoirs, tubes and platinum wires (see Figure 4-4). The reservoirs contained up to 40 µl of liquid. The liquid flows through the biochip using either air pressure on the tubes or by electricity applied to the platinum wires.

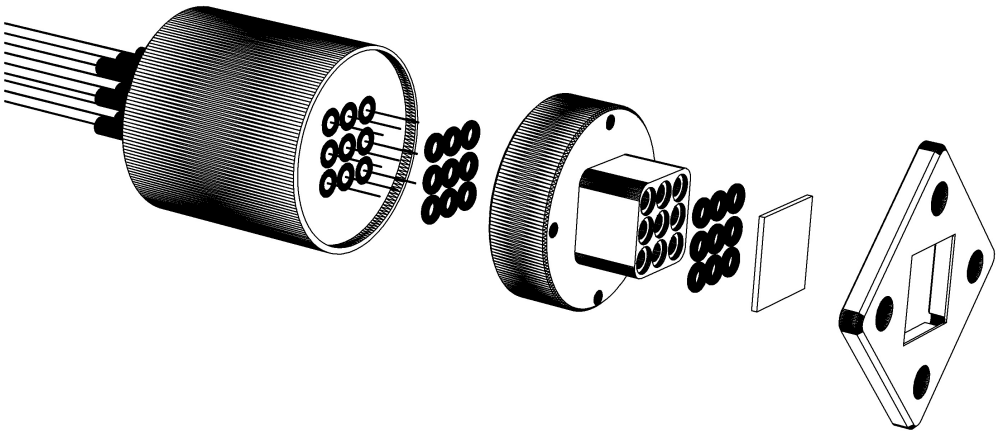

Figure 4-4. Exploded view of the biochip holder. From left to right: Polymer block containing platinum wires through small tubes, set of O-rings, reservoirs, set of O-rings, biochip and aluminium end-plate.

The assembled device was placed in a piezo-controlled microscopic xyz translation stage (PiezoJena, Jena, Germany). With this translation stage the biochip can be moved 80 µm in all three directions with at least 100 nm precision and reproducibility. The confocal detection system consisted of an inverted fluorescence microscope (ConfoCor I, Carl Zeiss, Jena, Germany), especially designed to perform fluorescence correlation spectroscopy (FCS) (Hink *et al.*, 2003; Kunst *et al.*, 2002). The 488 nm line from an argon laser was used to excite fluorescent molecules (Rhodamine Green, Rhodamine Green labelled dextrans) and fluorescent microspheres. Neutral density

filters were used to decrease incident laser power when needed. Fluorescence photons were detected by an avalanche photodiode (EG&G, Quebec, Canada) and autocorrelated in real time by an ALV-5000 computer card (ALV, Langen, Germany) in a standard Windows based computer. ConfoCor I software was used to control this card and to store FCS data.

Generation and control of electric fields

An electric field was applied to the microchannels to drive liquid or particles forward. Electric field strengths up to 500 $V.cm^{-1}$ were sufficient. Platinum electrodes from the biochip were attached to a computer controlled High Voltage (HV) relay bank. The electric fields were generated using several HV-modules obtained from UltraVolt (Ronkonkoma, Long Island, NY, USA). The HV-output from these modules can be any value between 0 and 2 kV. They take a control input of 0 - 5 V.

A digital-to-analogue computer card (NI-6711, National Instruments Corporation, Austin, Texas, USA) controlled the output of the modules in combination with a homemade Labview (National Instruments Corporation) program. The analogue outputs of this card can be programmed to be between 0 and 10 V and are fed into the HV-modules. Since the HV-modules were not protected against wrong inputs, some additional components were added. The resistor divider halved the output of the D/A card while the diode protected against wrong polarity (see Figure 4-5).

Fast switching (ms range) HV relays (R1329, Celduc, Sorbiers, France) were used to switch power from different HV-modules to the biochip electrodes. Switching the flow to different reservoirs was used to sort particles. The electrodes can be connected to one of the HV power supplies, to electrical ground or to nothing (floating). As a quality control parameter during experiments, the electrical current through the biochip electrodes was monitored using the current sense output from the HV-modules. This output was fed into a differential input of an analogue-to-digital converter computer card (NI-6023E, National Instruments Corporation). After calibration the output values were shown inside the same Labview program that drives the HV-modules.

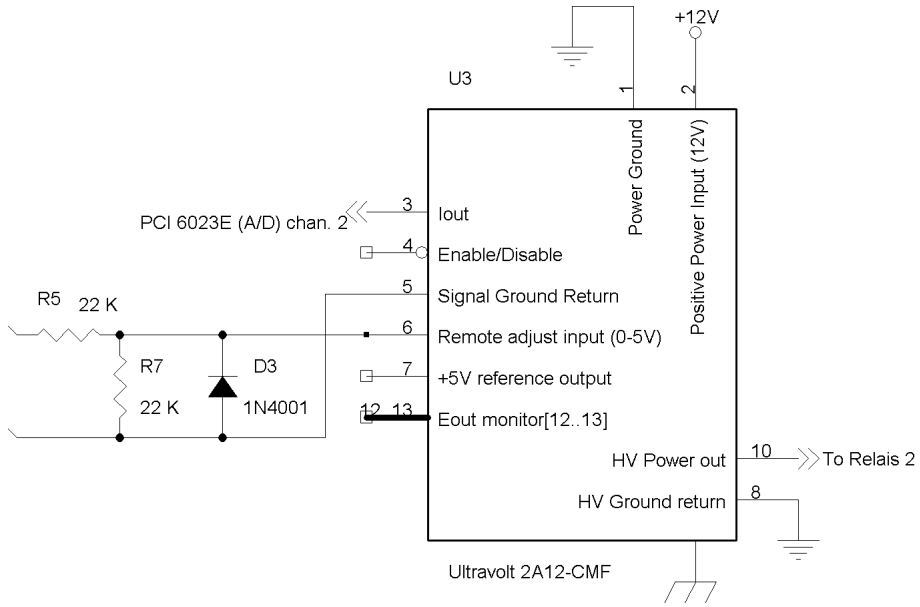

Figure 4-5. Excerpt from HV power supply schematic diagram showing a protected input by a resistor- and diode-network.

Experiments

Real time detection and subsequently sorting of flowing fluorescent particles

When a fluorescent particle passes through the confocal observation volume a burst of photons is emitted. A burst is defined as a minimum of x photons within a discrete time window of y seconds (typical values for x and y are 100 and 0.02, respectively). These bursts have different characteristics as compared to the background signal. The longer a particle resides in the observation volume, the more photons are emitted. This residence time is obviously correlated with the flow velocity of the particle and the size of the observation volume. The amount of photons can be estimated in a typical experiment for green-yellow microspheres (Haugland, 2002) (ø = 1 µm) exposing ~150x10^3 fluorescent molecules (brightness of 16x10^3 photons.s^{-1}.molecule^{-1}) and transiting through the observation volume for 20 ms. This number amounts to ~336x10^3 photons within this time period

assuming an overall system detection efficiency of 0.007 using a 20x objective (Plan Neofluor, NA=0.5, Zeiss, Jena, Germany). The background signal in this time window with this objective is normally less than 20-30 photons.

The burst detection electronics consisted of two Complex Programmable Logic Devices (CPLD) (EPM7512AE, Altera, San Jose, CA, USA) coupled to a microcontroller (C167CR, Infineon Technologies AG, Munich, Germany). These CPLDs performed several tasks like real-time detection, pipelining of positives and driving the HV relays to sort the particles. These tasks are briefly addressed below.

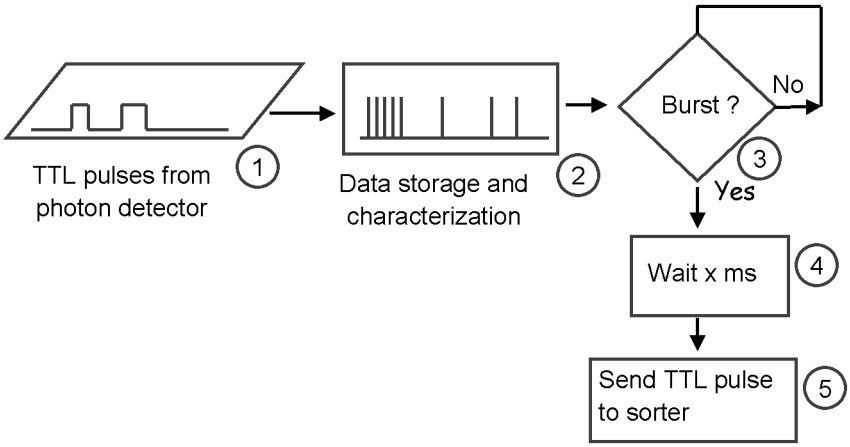

Figure 4-6. Flowchart of burst detection.

The TTL output from the avalanche photodiode was connected to one of the CPLDs. This is represented by step 1 in Figure 4-6. The microcontroller programs the CPLDs with information needed for real-time detection (time window, minimal number of photons within this time window) as well as timing parameters involved for sorting. Inside the CPLD the photons are time-stamped (step 2). When a positive burst is detected (step 3), the CPLD gives a delayed (step 4) signal to the HV relays (step 5). This delay is needed since there is a time difference (because of the finite path length) between the point of detection and the channel junction for sorting. The delay and pulse duration is programmable. Since there can be more than one particle detected before sorting, a pipeline (steps 4 and 5) is included in the CPLD design. The capacity of the pipeline is circa 30 – 40 detection and sorting events per second.

Two of these detection systems were NANDed together to create a detection system that is capable of coincidence detection of two different fluorescent photon bursts (Yeng *et al.*, 2003). This is useful for dual-colour fluorescent labelling strategies.

Electro-osmotic flow in the biochip measured with fluorescence correlation spectroscopy

Buffers of low ionic strength or salt solutions (< 50 mM) can be pumped through the channels using either electric fields or pressure. Concerning generation of liquid flow by electricity it should be realized that the glass wall is negatively charged; positive ions from the liquid are attracted to this surface. An electric field will move these ions to the cathode thereby dragging the solution with them. This phenomenon is called electro-osmotic flow (EOF) and is influenced by the buffer composition (ionic strength and type of ions) (Chankvetadze, 1997). EOF can only be applied in channels smaller than ~100 μm. The flow velocity of fluorescent molecules or particles through the channel can be determined with FCS as described previously (Dittrich and Schwille, 2002; Kunst *et al.*, 2002). Thus, a focused laser beam together with confocal detection optics was used to probe a tiny observation volume having a Gaussian 3D intensity profile (~ Ø 0.5 by 3 μm) inside the channel. Only those fluorescence photons emitted in the observation volume were detected and autocorrelated in real-time yielding an autocorrelation curve. This autocorrelation curve contains information about diffusion rate and flow velocity of the fluorescent species. The theoretical framework of FCS in the analysis of uniform translation and laminar flow, superimposed on diffusion and active transport, have been given by Magde *et al.* (1978). In our case, the flow-FCS model was slightly adjusted to account for short-term phenomena like triplet-state kinetics of the molecules (Widengren *et al.*, 1995). When there is active transport in the form of laminar flow (i.e. not turbulent), the autocorrelation function $G(\tau)$ changes to (Brinkmeier *et al.*, 1999; Brinkmeier and Rigler, 1995; Gösch *et al.*, 2000; Kunst *et al.*, 2002):

$$G(\tau) = 1 + \frac{B}{N} \cdot A \cdot e^{-\left[\left(\frac{\tau}{\tau_{flow}}\right)^2 \cdot A\right]} \qquad (4\text{-}1)$$

where

$$A = \left(1 + \frac{\tau}{\tau_{diff}}\right)^{-1} \cdot \left[1 + \left(\frac{\omega_{xy}}{\omega_z}\right)^2 \cdot \left(\frac{\tau}{\tau_{diff}}\right)\right]^{-\frac{1}{2}}$$

and

$$B = 1 + \frac{F_{trip}}{1 - F_{trip}} \cdot e^{-\frac{\tau}{\tau_{trip}}}$$

In Eq. 4-1 N denotes the number of fluorescent particles in the confocal observation volume (COV), τ_{flow} is the flow time, τ_{diff} is the diffusion time of the fluorescent particle (or its residence time in the COV), ω_{xy} and ω_z are the radius and length of the COV, respectively, assuming that the spatial intensity distribution of the laser beam has a Gaussian 3D-profile. F_{trip} and τ_{trip} are the fraction of the molecules in the triplet state and the lifetime of the triplet state, respectively.

The flow velocity v is given by:

$$v = \frac{\omega_{xy}}{\tau_{flow}} \qquad (4\text{-}2)$$

10 nM Rhodamine Green labelled 70kD dextran was used in the flow experiments since this molecule has a relatively high molecular weight. This means that the influence of passive diffusion ($D_{trans} = 3.05 \times 10^{-11}$ $m^2.s^{-1}$) on the autocorrelation curve was minimized yielding a clear dependence on the flow

velocity. The buffer consisted of 10 mM sodium tetraborate in water (pH=9.1). The 488-nm line of an argon laser was focused in the middle of a 50 x 20 μm (height x depth, respectively) channel of a biochip with a 40x, NA=1.2 water immersive objective (apochromat, Zeiss, Jena, Germany). The laser intensity was attenuated to approximately 40 μW with a neutral density filter. Electrical field strengths ranging from 0 V to 275 V.cm^{-1} has been used. The measured FCS curves showed a clear dependence on the electrical field strength. Higher electric fields displaced the autocorrelation traces to shorter times (see Figure 4-7). These FCS traces were analyzed using the earlier described flow-FCS model (Chapter 2) to obtain flow velocities (see Table 4-1). The flow velocity of the liquid in the middle of the microchannel due to EOF is plotted in Figure 4-8. The curve deviates from linearity at higher flow velocities due to leakage to the other open channels in the chip.

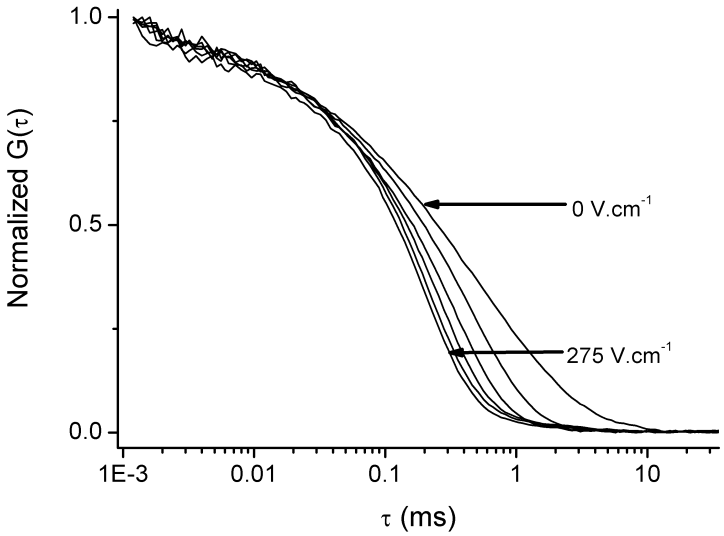

Figure 4-7. Normalized autocorrelation curves (average of ten curves each collected during 10 s) of 10 nM Rhodamine Green labelled dextran (70 kD) flowing through a microfluidic channel due to electro-osmotic flow. Curves from right to left: 0 V.cm^{-1} to 275 V.cm^{-1} with incremental steps of circa 55.5 V.cm^{-1}.

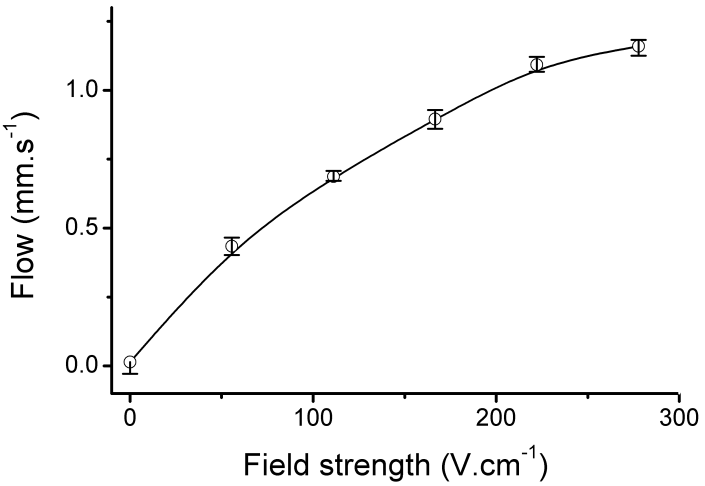

Figure 4-8. Electro-osmotic flow in a biochip. The flow velocity of 10 nM Rhodamine Green labelled dextran (70 kD) in the middle of a 50x20 μm channel depends on the applied potential difference.

Field strength $V.cm^{-1}$	τ_{diff} ms	Confidence Interval (67%)	τ_{flow} ms	Confidence Interval (67%)	V $mm.s^{-1}$	Confidence Interval (67%)
0	0.321	0.312 – 0.331	20	5 – n.f.	0	
56	0.262	0.249 – 0.274	0.651	0.606 – 0.701	0.43	0.40 – 0.46
111	0.245	0.235 – 0.254	0.412	0.403 – 0.425	0.69	0.67 – 0.71
167	0.239	0.225 – 0.252	0.316	0.304 – 0.328	0.90	0.85 – 0.93
222	0.230	0.217 – 0.244	0.259	0.253 – 0.266	1.1	1.1 – 1.1
278	0.241	0.231 – 0.253	0.244	0.237 – 0.249	1.2	1.1 – 1.2

Table 4-1. Analysis of autocorrelation traces of a 70kD-dextran labelled with Rhodamine Green using the triplet-flow-fcs model. The following parameter values were obtained at a field strength of 0 $V.cm^{-1}$ (no flow): $F_{triplet} = 0.15$, $\tau_{triplet} = 2.0$ μs and a structure parameter of 5. The values of triplet and structure parameters were fixed during the analysis of autocorrelation traces in case of flow. The values of the confidence interval are obtained after a rigorous error analysis at the 67% confidence level. n.f.: upper limit not found.

Real-time detection and sorting of flowing fluorescent microspheres

In contrast to the previous experiment where the flow velocity was determined off line from analysis of autocorrelation curves, it was desirable to measure the microsphere velocity in real time in order to facilitate the HV- and time-delay settings of the biochip for proper operation. For this purpose larger fluorescent particles were used. Fluorescent green-yellow microspheres or beads (diameter circa 1 μm; F8823, Molecular Probes, Leiden, The Netherlands) were suspended in buffer (10 mM sodium tetraborate, 0.03 % Tween-20, pH=9.1). The non-ionic detergent Tween-20 was added to suppress EOF to ensure that movement of the beads in an electric field was only due to their electric charge. The biochip (width 50 μm; depth 20 μm) was flushed with buffer and the sample reservoir filled with the suspension of beads. The electrical field strengths were at the sample -160 $V.cm^{-1}$, focusing channels –370 $V.cm^{-1}$ and the sorting channel 530 $V.cm^{-1}$. With these parameters, the negatively charged beads were focused into a tiny stream and deflected to the collecting reservoir. Approximately 20 particles per minute were flown through the channel. The average particle velocity was determined using an intensified CCD camera (XTI, Photonics Science, East Sussex, UK) coupled to a frame grabber (Hercules 3D Prophet All-in-Wonder 9000pro, Guillemot Corp., La Gacilly Cedex, France). A mercury lamp was used for illumination through the aforementioned 20x objective; spectral excitation and emission filters inside the microscope ensured that only fluorescence of the particles were imaged on the CCD. Moving particles were captured and analyzed using movie software (Premiere, Adobe Systems Inc., Seattle, WA, USA). The average particle velocity was found to be 0.4 $mm.s^{-1}$ using the above-mentioned electrical field strengths.

Once the velocity was determined, sorting the beads proved to be feasible. The 20x optical objective used in the ConfoCor 1 created an illumination volume that excited practically all focused flowing microspheres in the microchannel. Particles were detected throughout the whole depth of the channel. Excitation came from the 488-nm line of the argon laser line combined with a tenfold attenuating neutral density filter resulting in 125 μW of light energy at the sample. In Figure 4-9 a typical photon burst is shown when one bead passed through the observation volume. The burst consisted of many photons emitted during transit. The burst detection threshold was set to 100 photons within a 3 ms time window. The output pulse was set to a small

delay (to easy visualize correlation between detection and output pulse) and a pulse width of 20 ms.

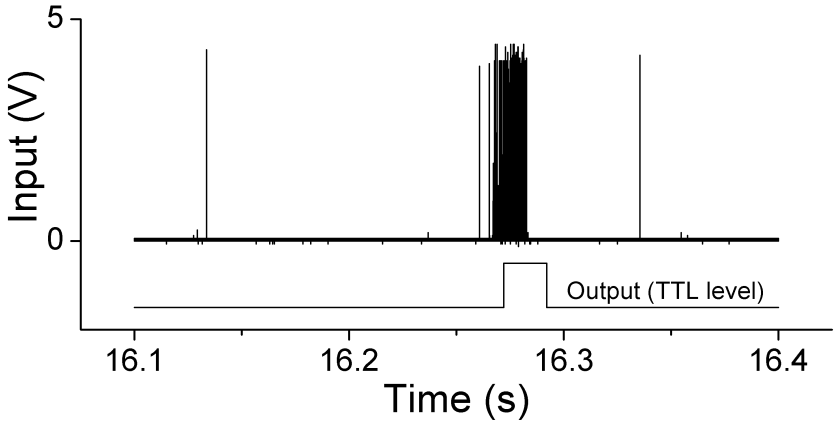

Figure 4-9. Real-time detection of a fluorescent microsphere. The top graph shows the real time output of the avalanche photodiode. This signal is attached to the detector logic. The lower graph shows the TTL output pulse (delay = 0.4 ms, width = 20 ms). It is connected to the reed relays logic.

Sorting of these 1-μm beads was demonstrated by connecting the output pulse to HV relays to switch between different collecting reservoirs. The output pulse was set according to the time needed for the particle to travel from the detection point to the channel bifurcation. It took, on average, 1.4 s for the particles to move from detection position to sorting point (0.6 mm). The output pulse was set to a delay of 1.2 s with a width of 0.4 s. With this scheme, fluorescent particles were collected in one reservoir similarly as described recently with fluorescence imaging using a CCD camera (Dittrich and Schwille, 2003) (data not shown). The sorting procedure was demonstrated to be stable for over a period of at least 2 hours.

Discussion

Liquid flow of relatively small fluorescent particles using electro-osmotic flow (EOF) in microchannels has been clearly demonstrated. However, EOF as a tool to propel and focus small particles proved not to be successful due to interference caused by the charge of the particles and the opposite direction of the fluid flow.

Addition of detergents to the buffer reduced the EOF. The particles then moved through the liquid solely based on their electrical charge. Fast switching HV reed relays turned out to be a successful method for sorting. The used beads had a uniformly negative charge, which resulted in a uniform velocity under the influence of an electric field.

Sorting of fluorescent particles starts with their detection. The detection depends on the brightness contrast between the particles and the background. The background was very low (< 5 photons per ms) compared to the signal. This is the reason why a medium power objective (20x, NA=0.5) has been used. It created an excitation volume that allowed the detection of highly fluorescent microspheres throughout the whole channel depth. Detection and subsequent sorting of fluorescent μm-sized particles could be demonstrated given the large photon bursts despite the lower light gathering power of this objective.

Preliminary experiments using fluorescent bacteriophages having sizes of 20 x 60 nm showed that it is more difficult to detect and sort these much smaller particles than the highly fluorescent beads. Because of a limited degree of labelling these bacteriophages possess much lower fluorescence brightness than the microspheres. Reducing the confocal observation volume (COV) using a higher numerical aperture objective allows detection of single phages. However, this size is substantially smaller than the width and depth of the channel enhancing the probability that passing particles are not detected. When particles pass through the COV, they will not only travel fully through it, but will also partially transit the beam. This will result in uneven burst sizes with some sizes below the detection threshold. Furthermore, the 2D particle focusing mechanism that is applied successfully for μm-sized beads is not working for these phages due to their small size. Possible solutions could be found in reduction of the channel dimensions (Foquet *et al.*, 2002; Foquet *et al.*, 2004), rapid scanning of the laser beam (Berland *et al.*, 1996; Levi *et al.*, 2003) or by using waveguides (Fu *et al.*, 2004; Tung *et al.*, 2004).

At present, the speed of detection and sorting is too low for practical use. If one wants to sort 10^5 – 10^6 particles from a biolibrary in a limited period of time, a different approach is required. One efficient approach would be the parallel use of thousands of microfluidic channels in a chip combined (Erickson and Li, 2004) with a sensitive spatial detection device such as an electron-multiplying CCD or the photon detectors directly integrated in the chip (Adams *et al.*, 2003). Real-time analysis of the fluorescence data can be

performed by e.g. Field Programmable Gate Arrays (FPGA's) instead of the simpler CPLD's used in this work. Switching electric fields to sort particles with the help of reed relays in multi-channel chips would not be practical, as their excessively large number would create interfacing problems. One solution would be integration of switching elements (e.g. field effect transistors) in the chip and addressing them in a multiplexed manner.

This microfluidic platform was designed to be a technology demonstrator for small particle sorting. The particles can even have a relatively low fluorescence yield that is compensated by longer interrogation times as compared to the ones used in conventional FACS machines. The microfluidic device allows screening and sorting of relatively small particles like fluorescent-labeled bacteria and viruses. Further research using these technologies to screen a small phage library is currently being undertaken in our laboratories.

Acknowledgements

The authors thank Prof. dr. Albert van den Berg (Mesa+, University of Twente, Enschede, The Netherlands) for valuable advice and Micronit (Enschede, The Netherlands) for biochip fabrication. Hans de Rooij and Ing. Jacob van Otten are thanked for constructing the chip holder and the burst detector. We appreciated stimulating discussions with Dr. Mark Hink. This research was supported by the Dutch Technology Foundation (STW, grant WBI 4797).

Appendix to chapter 4

Supplementary information

Detection and sorting of fluorescent microspheres

Green-Yellow fluorescent microspheres (1 μm diameter, F8823, Molecular Probes, Leiden, The Netherlands) were suspended in buffer consisting of 10 mM sodium tetraborate, 0.03% Tween-20, pH=9.1. The number of fluorescent molecules on the surface of a microsphere is estimated to be approximately $150x10^3$. Fluorescence detection of these bright microspheres should then be very easy. The non-ionic detergent Tween-20 suppresses electro-osmotic flow. Therefore the negatively charged microspheres move through the stationary buffer, when an external electric field is applied. A biochip (Figure 4-2) was flushed at least 10 times with buffer using a vacuum pump. After the chip was placed in the holder (Figure 4-4), all reservoirs were filled with buffer except for one, which was filled with the sample. Care was taken not to introduce any air bubbles or foam in the microchannels and reservoirs as they interfere with the correct functioning of the system.

Electric potentials were applied at point A (400V) and C or D (switched between electrical ground and floating) (see Figure 4-10). At points B, the applied potential was 0 volt. The other channels were not connected to a high voltage and remained 'floating'. The B channels are called 'focussing channels'. The microspheres enter the channel at point A and are dispersed throughout the channel. At the intersection marked with a *, the microspheres are focussed into the middle of the channel. They also move towards the positive electrode faster than they did before the * intersection. Figure 4-10 is a 40-ms frame snapshot taken from a movie captured using fluorescence imaging. Slow moving microspheres are seen as round white dots and the faster ones are depicted as an elongated dot (stripe). The measured velocity was approximately 0.4 $mm.s^{-1}$. Circa 20 particles were flown through the channel per minute using this setup.

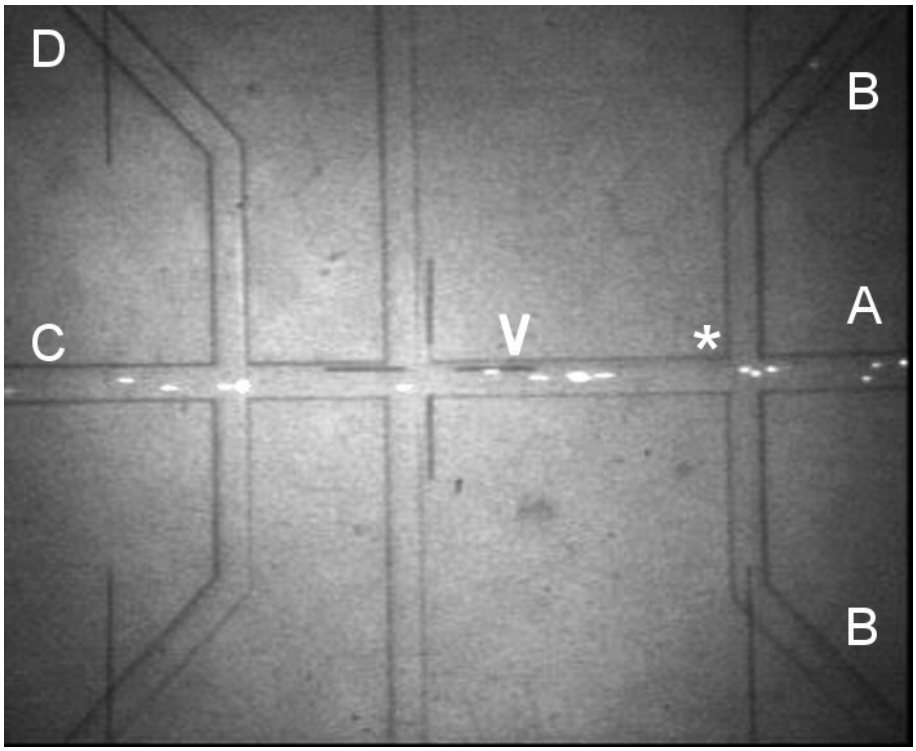

Figure 4-10. Fluorescence image of the biochip using a mercury lamp as excitation source combined with appropriate excitation and emission filters. The microspheres are focussed into a tiny spatial stream at the intersection between channel A and B (depicted with a *). The detection of flowing beads takes place at point V.

The 488-nm line from an argon laser was used to excite the fluorescent microspheres. When a fluorescent microsphere is detected at point V (see Figs. 4-10 and 4-11), the HV relays switch during a short time period to capture the microsphere. The captured beads are stored in the D channel as can be seen in Figure 4-12. The detection and sorting in this experiment was stable of a period of several hours. Thousands of microspheres were sorted in this manner.

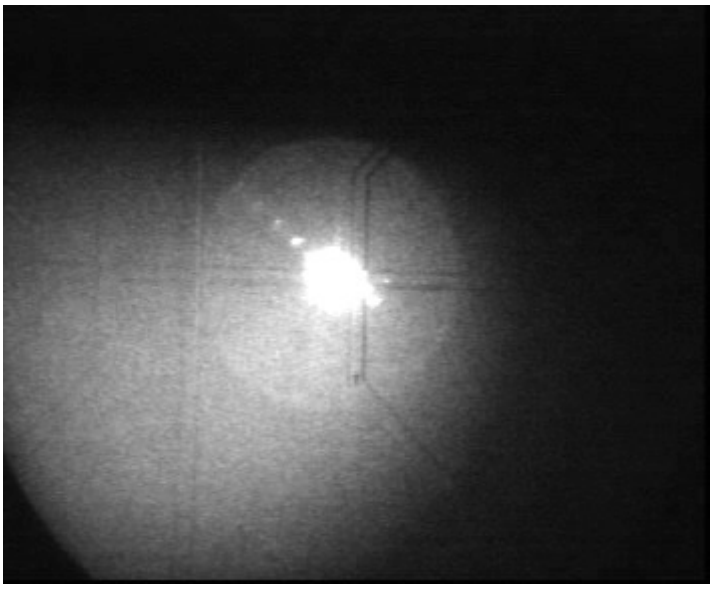

Figure 4-11. A fluorescent bead emits a bright flash of light when it passes through the laser spot. This burst of light is detected by the avalanche photodiode and triggers a sequence of sorting events that capture the bead.

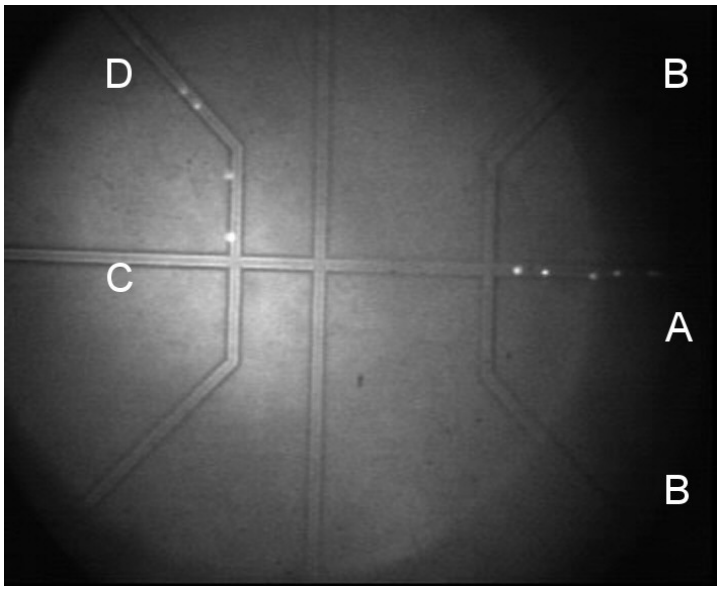

Figure 4-12. Fluorescence image of captured microspheres in channel D.

Bacteriophages in the biochip - detection and sorting

The goal of this study was to find out if and how single phages could be detected and sorted. This is of great importance for screening of bacteriophage-based biolibraries. One of the main concerns is the amount (or lack thereof) of fluorescence photons available from each single phage. The T7 bacteriophage is very small (Figure 4-13). We have studied T7 phages, which were externally labeled with Alexa Fluor™ 488 succinimidyl ester, because this fluorescent molecule is photostable, very bright, pH-insensitive and can be excited by the 488-nm line of an argon ion laser (Haugland, 2002).

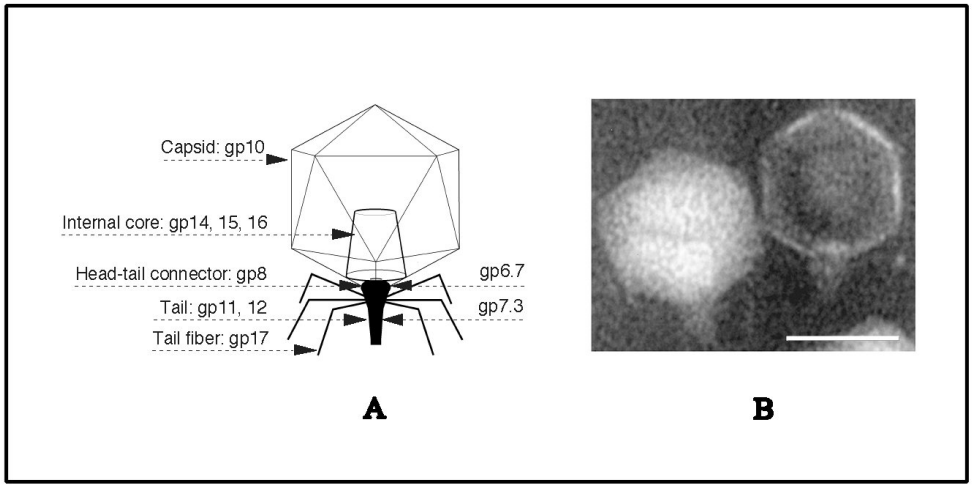

Fig 4-13. The T7 bacteriophage is a member of the *Podoviridae* family and preys upon various strains of *Escherichia coli*. Its tail recognises and attaches to *E. coli* and injects its DNA, which is packed inside the capsid shell, through the tail into the bacterium. After about 25 minutes (30 ºC), around hundred new lytic bacteriophages burst from the bacterium.
A: Schematic representation of the T7 phage indicating its protein composition.
B: Electron microscopy image: Courtesy of S. Adhya and D. Scholl (www.thebacteriophages.org). Bar = 50 nm.

T7 Phages (t7select10b, Novagen, USA, $2x10^8$ phages.μl^{-1} in 0.1 M $NaHCO_3$ (pH=8.3)) were obtained from Hans Keller (Laboratory of Molecular Recognition and Antibody Technology, Wageningen University, The Netherlands). Labelling of the phages was performed as follows: 200 µl phages were slowly stirred with 5 µl Alexa 488 carboxylic acid, tetrafluorophenyl ester (10 $\mu g.\mu l^{-1}$ in DMSO) (A20181 conjugation kit, Molecular Probes Europe BV,

Leiden, The Netherlands) in the dark at room temperature. After 1.5 hours the reaction was stopped by addition of 100 µl (100 $mg.ml^{-1}$) hydroxylamine (pH=8.5). Slow stirring continued for 1 hour in the dark. The labelled phages were purified using the supplied purification filter (30 kD size exclusion filter) with PBS, pH=7.2. FCS experiments using the ConfoCor-1 instrument (Carl Zeiss, Jena, Germany; excitation with 488-nm laser attenuated to 38.2 µW and emission detected through proper dichroic and band pass filters) showed only fast moving dye in these samples. Apparently, there was still Alexa dye absorbed to the phages, which slowly releases into the solution. To remove this unwanted absorbed dye, the samples were filtered 10 times using 30 kD cut-off miniature spin columns using chip-buffer A (50 mM tris, 50 mM NaCl, 0.03% Triton X100, pH=8.0). After these washing steps, FCS curves showed only fluorescent phages (Figure 4-14) and no dissolved dye. The conjugated phages were collected in 100 µl chip-buffer A. The final phage concentration was approximately $2x10^{6}.\mu l^{-1}$ as determined by a viability count (determined by H. Keller).

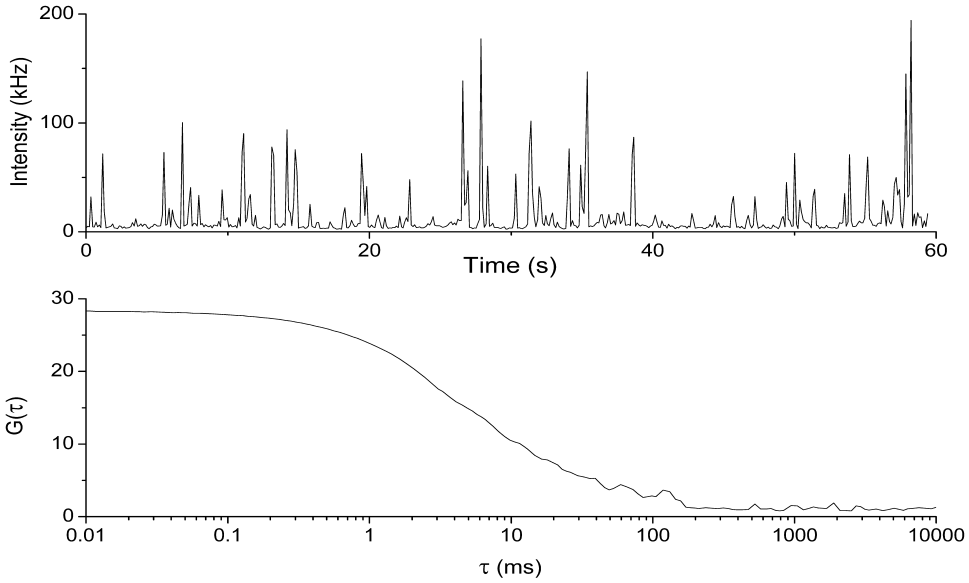

Figure 4-14. Intensity trace (top) (of one representative experiment) and fluorescence autocorrelation curve (bottom) of T7 bacteriophage conjugated with Alexa-488 after 11 rounds of purification. This curve is the average of 18 experiments, each lasting 60s. The diffusion time of the bacteriophages is 4.95 +/- 0.15 ms.

Fluorescent-labelled T7 phages show spikes of photons ranging from 30 to 200 kHz (see Figure 4-14 top panel). Under similar experimental conditions 6.8×10^3 photons.s^{-1} were detected from *one* Alexa 488 molecule. Thus there were approximately 25 Alexa molecules per phage. The physical size of the phages can be estimated from these experiments using the Stokes-Einstein relation relating the translational diffusion coefficient, D_{trans} , of the particle with its hydrodynamic radius, R_H : $D_{trans} = kT/(6\pi\eta R_H)$, where k is the Boltzmann constant (1.3807×10^{-23} J.K^{-1}), T is temperature (K), η is the dynamic viscosity of the solvent (1.0016×10^{-3} kg.m^{-1}.s^{-1}). The translational diffusion coefficient D_{trans} is related to the diffusion time τ_{diff} via $D_{trans} = \omega_{xy}^2/4\tau_{diff}$, where ω_{xy} is the radial width (in m) at $1/e^2$ of the intensity maximum of the cofocal volume beam-waist. ω_{xy} is obtained through calibration of the whole instrument (see chapter 2). Normally it is in the range of half the wavelength of the used laser light. Alexa 488 has a D_{trans} of 3×10^{-10} m^2.s^{-1} (Kim and Schwille, 2003) yielding the ω_{xy} for the instrument. Using D_{trans} for Alexa488-T7 phages, the hydrodynamic radius for the phages is calculated to be 60 nm, which is in very good agreement with the electron micrograph dimension shown in Figure 4-13.

Channel dimensions

The bacteriophages are very small (hydrodynamic radius ~ 60 nm). They would not perform well in large 50 μm wide channels. Therefore smaller channels are needed. Small channels cannot be fabricated using Pyrex™ since this material etches in an anisotropic fashion. Etching to a depth of 10 μm will result in a width of 25 μm when using a mask with 5 μm line width. The channels need a minimum depth of 10 μm because the confocal laser spot has an axial length of a few micrometers. The laser spot or confocal volume element needs to be completely immersed in the liquid and should not touch the liquid-glass boundary, since otherwise the CVE is not well defined and detection artefacts will occur. A large channel depth is not recommended when dealing with nm-sized particles. A compromise had to be made.

Chips with channel widths ranging from 5 to 20 μm and depths of 10 or 20 μm in fused silica have been made by Micronit (Enschede, The Netherlands) using a DRIE (Deep Reactive Ion Etching) method.

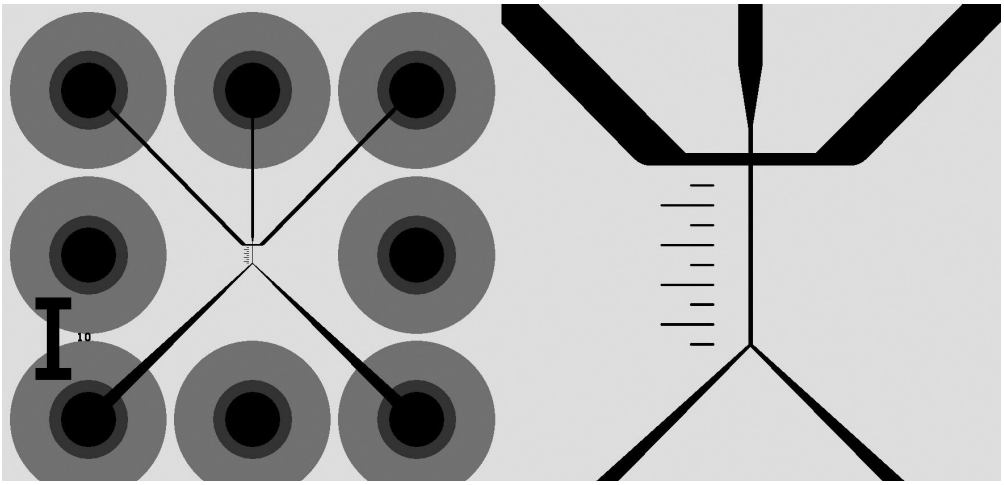

Fig 4-15. **Left**: Excerpt of a chip design with a 10 μm wide detection channel. The round spheres represent the liquid reservoirs. The top right and left reservoirs connect to the focus channels. The top middle reservoir holds the sample. The two reservoirs at the bottom are used to collect waste and sorted particles.
Right: Detail of the centre part of the chip. The major ruler divisions have a length of 100 μm. The minor divisions are 50 μm. The small channel has a width of 10 μm.

Concluding remarks

Fluorescently labelled phages were flown through the chip using a potential difference of 30 - 100 V between the main channel and the output. The used buffer (chip buffer A, see above) suppressed electro osmotic flow; phages are propelled due to their negative electric charge. As anticipated, the observed fluorescence was low and the phages could only be seen using an image intensifier attached to the video camera. Unfortunately it was not possible to focus the phages into a tiny stream using a chip with a channel width of 5 μm. The phages are too small for these relative large channels and therefore most of them pass undetected. However, about 3000 single phages were detected during a 3-hour period. Sorting of phages could not be established using this setup.

Chapter 5

Summarizing discussion

To unravel protein interaction patterns peptide and cDNA libraries displayed on bacteriophages can be used. Recent developments in optical imaging technology and in expression and labelling strategies enable specific and sensitive selection of peptides and proteins from peptide and cDNA libraries expressed on phage or bound to a solid surface as used with arrays. It has now been shown that overexpression of cDNAs in expression vectors using cell microarrays can be used to identify genes in various cellular processes (Howbrook *et al.*, 2003; Wu *et al.*, 2002). Many applications of cDNA phage display have been reported, including the isolation of serine protease inhibitors, lectins, lysosomal proteins, allergens, antigens, proteins involved in various signalling pathways and many more. To elucidate protein interaction networks and signalling pathways, important information can also be derived from peptide libraries (Turk and Cantley, 2003). Peptide library approaches can be broadly grouped into methods employing either synthetic or encoded libraries. Synthetic libraries are bound to a solid support such as beads or microarrays. In many screening strategies fluorescent receptor proteins are being used. Encoded libraries are usually displayed in bacteriophages. In most of the studies applying phage display, panning procedures or variations thereof have been used for selecting genes encoding interacting proteins. Several rounds of selection are usually required to end up with a number of phage clones with a high selectivity (Christensen *et al.*, 2001; de Wildt *et al.*, 2000). Apart from this time-consuming process the whole protocol may result in a loss of rarely expressed genes and of genes encoding proteins having a lower affinity for the bait protein. Interesting genes may thus be lost. Therefore, novel sensitive fluorescence methods may facilitate the development of new selection strategies. These methods are based on single-molecule fluorescence detection and the use of microfluidic devices.

The same confocal fluorescence microscopy techniques for cellular imaging can be used for screening and sorting of biolibraries. Thereto, it is necessary to develop optimum contrast schemes between the reporting fluorescence signals and the non-desired background signals resulting in the highest level of sensitivity, precision and speed of measurements, temporal

and spatial resolution. In the last couple of years there has been considerable interest in using microfabricated devices for a variety of (bio)chemical processes (Dittrich and Manz, 2005, 2006; Dittrich *et al.*, 2006; Janasek *et al.*, 2006). Microfluidic devices are composed of micrometer channels and microliter reservoirs that are capable of transferring and storing tiny amounts of liquids in volumes of nano- and picoliters. Integrated microfluidic systems combine channels of microscopic geometry with miniaturized pumps, mixers, valves, electric components and light detectors. Miniaturization is one of the key technology concepts of current high-throughput screening systems. Miniaturization offers various advantages over macro-scale laboratory operation: (i) reduced sample volume and less reagents thereby reducing the costs of reagents, (ii) faster reactions and reagent mixing are possible, (iii) superior heat and mass transfer eliminating thermal side-effects, (iv) more accurate measurements, (v) low-cost compact system design in which more functionalities can be integrated or operated in parallel. Much progress has been made in the development of materials needed to make microfluidic devices and the various ways to direct liquid flow inside microchannels. The fluid is usually driven by pressure, vacuum or by electrical fields (EOF, electro osmotic flow). The direction of fluid flow can be diverted by various methods such as mechanical valves or by changing voltage gradients over different channels. Electrically charged particles can be moved in a stationary liquid (EOF suppressed) using DC electric fields or AC fields (dielectrophoresis).

The objective of the research described in this thesis was to design a microfluidics platform for the screening of biolibraries. This microfluidic platform can be considered as a technology demonstrator for the screening and sorting of particles which are smaller than cells like fluorescent-labelled beads, bacteria and viruses. The particles can even have a relatively low fluorescence yield that can be compensated by longer interrogation times as compared to the ones used in conventional flow cytometry that is now capable of screening many thousands of cells per minute.

In chapter 2 capillary flow experiments are described with fluorescent molecules, bacteria and microspheres using fluorescence correlation spectroscopy as an analytical tool. A diluted solution of fluorescent particles is flown through the square microcapillary (length 100 μm) and the fluorescence fluctuations are measured. The flow velocity is determined by fitting autocorrelation traces with a model containing parameters related to diffusion and flow. The flow profile of pressure-driven flow inside a microcapillary

is also determined by analyzing the fluorescence fluctuations of a small fluorescent dye. It was found that bacteria and microspheres are anomalously retarded in their flow by optical forces produced by the laser beam. Brister *et al.* (2005) have critically assessed these results. These authors postulated that the retardation was not due to optical forces but to detector saturation. However, the visible trapping of large particles observed at high laser power was not discussed by these authors (Brister *et al.*, 2005). Simulations have shown that under conditions of detector saturation the autocorrelation curve is flattened, thereby increasing the found diffusion times. The solution is to have a constant photon flux on the detector by using a variable neutral density filter in front of the detector. Unfortunately, this was not possible to implement in the commercial ConfoCor 1 microscope.

In chapter 3 the current achievements in generation of biolibraries, single-molecule detection techniques and microfluidic devices are separately discussed in the context of developing new screening technologies for biolibraries. The selection of specific binding molecules like peptides and proteins from biolibraries using, for instance, phage display methods can be quite time-consuming. It is therefore desirable to develop a strategy that is much faster in selection and sorting of potential binders out of a biolibrary. A high-throughput microfluidic platform is then proposed that combines the propulsion fluorescent components of the biolibrary through microchannels, single-molecule fluorescence photon burst detection and real-time sorting of positive hits.

In chapter 4 an instrumental system is described for detecting and sorting single fluorescent particles such as microspheres, bacteria, viruses or even smaller macromolecules in a liquid. The system consists of microfluidic chips, computer controlled high voltage power supplies, and a fluorescence microscope with confocal optics. The confocal observation volume and detection electro-optics allow measurements of single flowing fluorescent particles. The output of the avalanche photodiode (single photon detector) is coupled to a real-time photon-burst detection device, which output controls the high voltage power supplies for sorting purposes. Liquid propulsion systems like electro-osmotic flow to direct the particles through the observation volume have been tested and evaluated. The detection and real-time sorting of fluorescent microspheres are demonstrated. In supplementary material the detection and real-time sorting of (strongly) fluorescent microspheres are successfully demonstrated. Based on supplementary experiments the limitations of these microfluidic chips for

screening of fluorescent bacteriophages are briefly discussed.

In summary, efficient particle sorting based on strongly fluorescent beads is now possible using the confocal microfluidic particle sorter. Fluorescent T7 bacteriophages can be propelled through microchannels using electric fields. However, focusing was not possible due to the relatively large width of the microchannel (5-10 μm) as compared to the size of the particle (50 nm). For interrogation of the fluorescent particles use is made of on-the-fly detection of fluorescence photon bursts. A burst is defined as a minimum of *x* photons within a discrete time window of *y* seconds (typical values for *x* and *y* are 100 photons and 20 milliseconds, respectively). The longer a particle resides in the excitation/observation volume, the more photons are emitted. This residence time is obviously correlated with the flow velocity of the particle and the size of the observation volume. The amount of detectable photons can be estimated in a typical experiment for a bacteriophage with *one* Yellow Fluorescent Protein (YFP) molecule on its surface and transiting through the observation volume for 20 ms. Suppose that the brightness of YFP amounts to 2 x 10^4 photons.s^{-1}.$molecule^{-1}$ (this is a realistic number). That will yield potentially 400 fluorescence photons. However, assuming an overall detection efficiency of 3% in confocal microscopy, the number of photons that will be detected is only 12, provided that there is no background noise. In addition, experiments have shown that it is very difficult to focus a flow of nanometer-sized particles through the middle of the channel where the laser beam is focused. Having a channel width and depth of 10 μm, a focal spot of 0.5 μm in diameter with a height of 2-3 μm (approximately), most 50 nm-sized phages will escape detection. One can then imagine that it will be difficult to track and deflect a singly labelled bacteriophage in solution. A drawback of these relatively small channel sizes is that they get clogged up quite easily with dust or even small glass splinters (from imperfect dicing of the chips).

Technical improvements can be made along the following lines. Nanofluidic (instead of microfluidic) devices will be realized in the very near future owing to improvement in fabrication processes and advances in nanoscale sensing and actuation (Mijatovic *et al.*, 2005). This will result in further downscaling of sorting and selection of biolibraries. An additional advantage is that fluorescence can be detected without the necessity to focus the particle stream (Foquet *et al.*, 2002; Foquet *et al.*, 2004). For a proper functioning of nanofluidic devices, techniques to control passage of the fluid as well as to determine the flow speed in minute volumina must be developed.

At present, the speed of detection and sorting of smaller particles is too low for practical use. If one wants to sort $10^5 – 10^6$ particles from a biolibrary in a limited period of time, novel methods must be developed such as the parallel use of many microfluidic or nanofluidic channels in a chip combined with a sensitive spatial detection device such as an microchannel plate enhanced CCD or photon detectors directly integrated in the chip. For library versus library screening one can use phages that are labelled with two spectrally different fluorescent labels and detection of coincidence photon bursts. The electronics developed with the current confocal particle sorter has the possibility to detect two channels simultaneously and creating a sorting pulse on coincidence. Coincidence photon burst methods allow the detection of femtomolar dual-labelled biomolecules in the presence of 1000-fold molar excess of single-labelled ones. The speed of data processing can be improved by developing not only better steering electronics and light collection optics but also appropriate real-time control analysis software. Finally, much effort will be spent in the design of optical biosensors that can provide a unique yes-no answer for positive hits.

Important applications are foreseen for a more rapid and reliable screening and sorting of biolibraries. This is necessary in this era of post-genomics where a rapid translation of gene sequences into gene and even cell function is of increasing importance. This not only allows us to rapidly process the wealth of information coming from the numerous genome-sequencing efforts, but also helps us to acquire insight in the functioning of protein machines and, as a consequence, cells. In the near future, high throughput fluorescence microscopy will play an important role in the way we perform cell biology. This so-called ‘systems biology’ is a holistic approach to (semi) real-time analysis of whole cells in the fields of e.g. functional genomics (Pepperkok and Ellenberg, 2006).

References

Adams, M.L., M. Enzelberger, S. Quake and A. Scherer. (2003). Microfluidic integration on detector arrays for absorption and fluorescence micro-spectrometers. *Sensors and Actuators A: Physical*, **104**(1): p. 25-31.

Agronskaia, A., J.M. Schins, B.G. de Grooth and J. Greve. (1999). Polarization effects in flow cytometric DNA sizing. *Applied Optics.*, **38**(4): p. 714-719.

Alberts, B. (1998). The cell as a collection of protein machines: Preparing the next generation of molecular biologists. *Cell*, **92**(3): p. 291-294.

Ambrose, W.P., P.M. Goodwin, J.H. Jett, A. Van Orden, J.H. Werner and R.A. Keller. (1999). Single molecule fluorescence spectroscopy at ambient temperature. *Chemical Reviews*, **99**(10): p. 2929-2956.

Andersson, H. and A. van den Berg. (2003). Microfluidic devices for cellomics: a review. *Sensors and Actuators B Chemical*, **92**(3): p. 315-325.

Applegate, R.W., J. Squier, T. Vestad, J. Oakey, D.W.M. Marr, P. Bado, M.A. Dugan and A.A. Said. (2006). Microfluidic sorting system based on optical waveguide integration and diode laser bar trapping. *Lab on a Chip*, **6**(3): p. 422-426.

Aragón, S.R. and R. Pecora. (1975). Fluorescence correlation spectroscopy and brownian rotational diffusion. *Biopolymers*, **14**: p. 119-138.

Aragón, S.R. and R. Pecora. (1976). Fluorescence correlation spectroscopy as a probe of molecular dynamics. *Journal of Chemical Physics*, **64**(15 February): p. 1791-1803.

Arifuzzaman, M., M. Maeda, A. Itoh, K. Nishikata, C. Takita, R. Saito, T. Ara, K. Nakahigashi, H.C. Huang, A. Hirai, K. Tsuzuki, S. Nakamura, M. Altaf Ul Amin, T. Oshima, T. Baba, N. Yamamoto, T. Kawamura, T. Ioka Nakamichi, M. Kitagawa, M. Tomita, S. Kanaya, C. Wada and H. Mori. (2006). Large-scale identification of protein-protein interaction of *Escherichia coli* K-12. *Genome research*, **16**(5): p. 686-691.

Ashkin, A. (1970). Acceleration and trapping of particles by radiation pressure. *Physical Review Letters*, **24**(4): p. 156-159.

Ashkin, A. (1992). Forces of a single-beam gradient laser trap on a dielectric sphere in the ray optics regime. *Biophysical Journal*, **61**: p. 569-582.

Ashkin, A. (1997). Optical trapping and manipulation of neutral particles using lasers. *Proceedings of the National Academy of Sciences of the USA*, **94**: p. 4853-4860.

Auer, M. (2001). HTS: understanding the physiology of life. *Drug Discovery Today*, **6**(18): p. 935-936.

Auroux, P.A., D. Iossifidis, D.R. Reyes and A. Manz. (2002). Micro total analysis systems. 2. Analytical standard operations and applications. *Analytical Chemistry*, **74**(12): p. 2637-2652.

Bacia, K. and P. Schwille. (2003). A dynamic view of cellular processes by in vivo fluorescence auto- and cross-correlation spectroscopy. *Methods*, **29**(1): p. 74-85.

Balla, S., V. Thapar, S. Verma, T. Luong, T. Faghri, C.H. Huang, S. Rajasekaran, J.J. del Campo, J.H. Shinn, W.A. Mohler, M.W. Maciejewski, M.R. Gryk, B. Piccirillo, S.R. Schiller and M.R. Schiller. (2006). Minimotif Miner: a tool for investigating protein function. *Nature Methods*, **3**(3): p. 175-177.

Beebe, D.J., J.S. Moore, J.M. Bauer, Q. Yu, R.H. Liu, C. Devadoss and B.H. Jo. (2000). Functional hydrogel structures for autonomous flow control inside microfluidic channels. *Nature*, **404**(6778): p. 588,589-590.

Beechem, J.M., E. Gratton, M. Ameloot, J.R. Knutson and L. Brand. The global analysis of fluorescence intensity and anisotropy data: second-generation theory and programs in *Topics in Fluorescence Spectroscopy*, vol: 2; J.R. Lakowicz, Editor. 1991, Plenum Press: New York.

Berland, K.M., P.T.C. So, Y. Chen, W.W. Mantulin and E. Gratton. (1996). Scanning two-photon fluctuation correlation spectroscopy: Particle counting measurements for detection of molecular aggregation. *Biophysical Journal*, **71**(1): p. 410-420.

Bianco, C., H.B. Adkins, C. Wechselberger, M. Seno, N. Normanno, A. De Luca, Y.P. Sun, N. Khan, N. Kenney, A. Ebert, K.P. Williams, M. Sanicola and D.S. Salomon. (2002). Cripto-1 activates nodal- and ALK4-dependent and -independent signaling pathways in mammary epithelial cells. *Molecular and Cellular Biology*, **22**(8): p. 2586-2597.

Bradbury, A., N. Velappan, V. Verzillo, M. Ovecka, L. Chasteen, D. Sblattero, O. Marzari, J.L. Lou, R. Siegel and P. Pavlik. (2003). Antibodies in proteomics I: generating antibodies. *Trends in Biotechnology*, **21**(6): p. 275-281.

Bradbury, A., N. Velappan, V. Verzillo, M. Ovecka, L. Chasteen, D. Sblattero, O. Marzari, J.L. Lou, R. Siegel and P. Pavlik. (2003). Antibodies in proteomics II: screening, high-throughput characterization and downstream applications. *Trends in Biotechnology*, **21**(7): p. 312-317.

Brinkmeier, M., K. Dörre, J. Stephan and M. Eigen. (1999). Two beam cross correlation: A method to characterize transport phenomena in micrometer-sized structures. *Analytical Chemistry*, **71**(3): p. 609-616.

Brinkmeier, M. and R. Rigler. (1995). Flow analysis by means of fluorescence correlation spectroscopy. *Experimental Technical Physics*, **41**(2): p. 205-210.

Brister, P.C., K.K. Kuricheti, V. Buschmann and K.D. Weston. (2005). Fluorescence correlation spectroscopy for flow rate imaging and monitoring - optimization, limitations and artifacts. *Lab on a Chip*, **5**(7): p. 785-791.

Butland, G., J.M. Peregrin Alvarez, J. Li, W.H. Yang, X.C. Yang, V. Canadien, A. Starostine, D. Richards, B. Beattie, N. Krogan, M. Davey, J. Parkinson, J. Greenblatt and A. Emili. (2005). Interaction network containing conserved and essential protein complexes in Escherichia coli. *Nature*, **433**(7025): p. 531-537.

Castro, A. and J.G.K. Williams. (1997). Single-molecule detection of specific nucleic acid sequences in unamplified genomic DNA. *Analytical Chemistry*, **69**(19): p. 3915-3920.

Chankvetadze, B. *Capillary electrophoresis in chiral analysis*. 1997, Baffins Lane, Chichester, West Sussex PO19 1UD, United Kingdom: John Wiley & Sons Ltd.

Chen, Y., J.D. Muller, P.T. So and E. Gratton. (1999). The photon counting histogram in fluorescence fluctuation spectroscopy. *Biophysical Journal*, **77**(1): p. 553-67.

Chou, C.F., R. Changrani, P. Roberts, D. Sadler, J. Burdon, F. Zenhausern, S. Lin, A. Mulholland, N. Swami and R. Terbrueggen. (2002). A miniaturized cyclic PCR device - modeling and experiments. *Microelectronic Engineering*, **61-2**: p. 921-925.

Chou, H.P., C. Spence, A. Scherer and S. Quake. (1999). A microfabricated device for sizing and sorting DNA molecules. *Proceedings of the National Academy of Sciences of the USA*, **96**(1): p. 11-13.

Chovan, T. and A. Guttman. (2002). Microfabricated devices in biotechnology and biochemical processing. *Trends in Biotechnology*, **20**(3): p. 116-122.

Christensen, D.J., E.B. Gottlin, R.E. Benson and P.T. Hamilton. (2001). Phage display for target-based antibacterial drug discovery. *Drug Discovery Today*, **6**(14): p. 721-727.

Cochrane, D., C. Webster, G. Masih and J. McCafferty. (2000). Identification of natural ligands for SH2 domains from a phage display cDNA library. *Journal of Molecular Biology*, **297**(1): p. 89-97.

Craighead, H.G. (2000). Nanoelectromechanical systems. *Science*, **290**(5496): p. 1532-1535.

de Folter, S., R.G.H. Immink, M. Kieffer, L. Parenicoca, S.R. Heinz, D. Weigel, M. Busscher, M. Kooiker, L. Colomo, M.M. Kater, B. Davies and G.C. Angenent. (2005). Comprehensive interaction map of the Arabidopsis MADS box transcription factors. *Plant Cell*, **17**(5): p. 1424-1433.

de Wildt, R.M.T., C.R. Mundy, B.D. Gorick and I.M. Tomlinson. (2000). Antibody arrays for high-throughput screening of antibody-antigen interactions. *Nature Biotechnology*, **18**(9): p. 989-994.

Dittrich, P.S. and A. Manz. (2005). Single-molecule fluorescence detection in microfluidic channels - the Holy Grail in mu TAS? *Analytical and Bioanalytical Chemistry*, **382**(8): p. 1771-1782.

Dittrich, P.S. and A. Manz. (2006). Lab-on-a-chip: microfluidics in drug discovery. *Nature Reviews Drug Discovery*, **5**(3): p. 210-218.

Dittrich, P.S. and P. Schwille. (2002). Spatial two-photon fluorescence cross-correlation Spectroscopy for controlling molecular transport in microfluidic structures. *Analytical Chemistry*, **74**(17): p. 4472-4479.

Dittrich, P.S. and P. Schwille. (2003). An integrated microfluidic system for reaction, high-sensitivity detection, and sorting of fluorescent cells and particles. *Analytical Chemistry*, **75**(21): p. 5767-5774.

Dittrich, P.S., K. Tachikawa and A. Manz. (2006). Micro total analysis systems. Latest advancements and trends. *Analytical Chemistry*, **78**(12): p. 3887-3907.

Dörre, K., S. Brakmann, M. Brinkmeier, K.-T. Han, K. Riebeseel, P. Schwille, J. Stephan, T. Wetzel, M. Lapczyna, M. Stuke, R. Bader, M. Hinz, H. Seliger, J. Holm, M. Eigen and R. Rigler. (1997). Techniques for single molecule sequencing. *Bioimaging*, **5**: p. 139-152.

Dörre, K., J. Stephan, M. Lapczyna, M. Stuke, H. Dunkel and M. Eigen. (2001). Highly efficient single molecule detection in microstructures. *Journal of Biotechnology*, **86**(3) Special Iss. SI): p. 225-236.

Drees, B.L. (1999). Progress and variations in two-hybrid and three-hybrid technologies. *Current Opinion in Chemical Biology*, **3**(1): p. 64-70.

Ehrenberg, M. and R. Rigler. (1974). Rotational brownian motion and fluorescence intensity fluctuations. *Chemical Physics*, **4**: p. 390-401.

Ehrenberg, M. and R. Rigler. (1976). Fluorescence correlation spectroscopy applied to rotational diffusion of macromolecules. *Quarterly Reviews of Biophysics*, **9**(I): p. 69-81.

Eigen, M. and R. Rigler. (1994). Sorting single molecules: application to diagnostics and evolutionary biotechnology. *Proceedings of the National Academy of Sciences of the USA*, **91**(13): p. 5740-5747.

El Karkouri, K., H. Gueune and C. Delamarche. (2005). MIPDB: a relational database dedicated to MIP family proteins. *Biology of the Cell*, **97**(7): p. 535-543.

Elson, E.L. and D. Magde. (1974). Fluorescence correlation spectroscopy. I. Conceptual basis and theory. *Biopolymers*, **13**: p. 1-27.

Enderlein, J. and M. Kollner. (1998). Comparison between time-correlated single photon counting and fluorescence correlation spectroscopy in single molecule identification. *Bioimaging*, **6**(1): p. 3-13.

Erickson, D. and D.Q. Li. (2004). Integrated microfluidic devices. *Analytica Chimica Acta*, **507**(1): p. 11-26.

Eriksson, T.L.J., O. Rasool, S. Huecas, P. Whitley, R. Crameri, U. Appenzeller, G. Gafvelin and M. van Hage Hamsten. (2001). Cloning of three new allergens from the dust mite *Lepidoglyphus destructor* using phage surface display technology. *European Journal of Biochemistry*, **268**(2): p. 287-294.

Fiedler, S., S.G. Shirley, T. Schnelle and G. Fuhr. (1998). Dielectrophoretic sorting of particles and cells in a microsystem. *Analytical Chemistry*, **70**(9): p. 1909-1915.

Foquet, M., J. Korlach, W. Zipfel, W.W. Webb and H.G. Craighead. (2002). DNA fragment sizing by single molecule detection in submicrometer-sized closed fluidic channels. *Analytical Chemistry*, **74**(6): p. 1415-1422.

Foquet, M., J. Korlach, W.R. Zipfel, W.W. Webb and H.G. Craighead. (2004). Focal volume confinement by submicrometer-sized fluidic channels. *Analytical Chemistry*, **76**(6): p. 1618-1626.

Fu, A.Y., H.P. Chou, C. Spence, F.H. Arnold and S.R. Quake. (2002). An integrated microfabricated cell sorter. *Analytical Chemistry*, **74**(11): p. 2451-2457.

Fu, A.Y., C. Spence, A. Scherer, F.H. Arnold and S.R. Quake. (1999). A microfabricated fluorescence-activated cell sorter. *Nature Biotechnology*, **17**(11): p. 1109-1111.

Fu, L.M., R.J. Yang, C.H. Lin, Y.J. Pan and G.B. Lee. (2004). Electrokinetically driven micro flow cytometers with integrated fiber optics for on-line cell/particle detection. *Analytica Chimica Acta*, **507**(1): p. 163-169.

Gandhi, T.K.B., J. Zhong, S. Mathivanan, L. Karthick, K.N. Chandrika, S.S. Mohan, S. Sharma, S. Pinkert, S. Nagaraju, B. Periaswamy, G. Mishra, K. Nandakumar, B.Y. Shen, N. Deshpande, R. Nayak, M. Sarker, J.D. Boeke, G. Parmigiani, J. Schultz, J.S. Bader and A. Pandey. (2006). Analysis of the human protein interactome and comparison with yeast, worm and fly interaction datasets. *Nature Genetics*, **38**(3): p. 285-293.

Gavin, A.C., P. Aloy, P. Grandi, R. Krause, M. Boesche, M. Marzioch, C. Rau, L.J. Jensen, S. Bastuck, B. Dumpelfeld, A. Edelmann, M.A. Heurtier, V. Hoffman, C. Hoefert, K. Klein, M. Hudak, A.M. Michon, M. Schelder, M. Schirle, M. Remor, T. Rudi, S. Hooper, A. Bauer, T. Bouwmeester, G. Casari, G. Drewes, G. Neubauer, J.M. Rick, B. Kuster, P. Bork, R.B. Russell and G. Superti Furga. (2006). Proteome survey reveals modularity of the yeast cell machinery. *Nature*, **440**(7084): p. 631-636.

Gavin, A.C., M. Bosche, R. Krause, P. Grandi, M. Marzioch, A. Bauer, J. Schultz, J.M. Rick, A.M. Michon, C.M. Cruciat, M. Remor, C. Hofert, M. Schelder, M. Brajenovic, H. Ruffner, A. Merino, K. Klein, M. Hudak, D. Dickson, T. Rudi, V. Gnau, A. Bauch, S. Bastuck, B. Huhse, C. Leutwein, M.A. Heurtier, R.R. Copley, A. Edelmann, E. Querfurth, V. Rybin, G. Drewes, M. Raida, T. Bouwmeester, P. Bork, B. Seraphin, B. Kuster, G. Neubauer and G. Superti Furga. (2002). Functional organization of the yeast proteome by systematic analysis of protein complexes. *Nature*, **415**(6868): p. 141-147.

Georgiou, G., ed. (2001) *Analysis of large libraries of protein mutants using flow cytometry*. Advances in Protein Chemistry. **55**: p. 293-315.

Georgiou, G., D.L. Stephens, C. Stathopoulos, H.L. Poetschke, J. Mendenhall and C.F. Earhart. (1996). Display of beta-lactamase on the *Escherichia coli* surface: Outer membrane phenotypes conferred by Lpp'-OmpA'-beta-lactamase fusions. *Protein Engineering*, **9**(2): p. 239-247.

Goll, J. and P. Uetz. (2006). The elusive yeast interactome. *Genome Biology*, **7**(6): p. 223.

Goodwin, P.M., M.E. Johnson, J.C. Martin, W.P. Ambrose, B.L. Marrone, J.H. Jett and R.A. Keller. (1993). Rapid sizing of individual fluorescently stained DNA fragments by flow cytometry. *Nucleic Acids Research*, **21**(4): p. 803-806.

Gösch, M., H. Blom, J. Holm, T. Heino and R. Rigler. (2000). Hydrodynamic flow profiling in microchannel structures by single molecule fluorescence correlation spectroscopy. *Analytical Chemistry*, **72**(14): p. 3260-3265.

Griep, R.A., C. van Twisk, J.M. van der Wolf and A. Schots. (1999). Fluobodies: green fluorescent single-chain Fv fusion proteins. *Journal of Immunological Methods*, **230**(1-2): p. 121-130.

Haugland, R.P. *Handbook of Fluorescent Probes and Research Chemicals*. 9th ed, ed. J. Gregory. 2002: Molecular Probes, Inc, Eugene, OR, USA.

Hell, S.W. (2003). Toward fluorescence nanoscopy. *Nature Biotechnology*, **21**(11): p. 1347-1355.

Hertzberg, R.P. and A.J. Pope. (2000). High-throughput screening: new technology for the 21st century. *Current Opinion in Chemical Biology*, **4**(4): p. 445-451.

Hess, S.T., S.H. Huang, A.A. Heikal and W.W. Webb. (2002). Biological and chemical applications of fluorescence correlation spectroscopy: A review. *Biochemistry*, **41**(3): p. 697-705.

Hink, M.A., J.W. Borst and A.J.W.G. Visser. (2003). Fluorescence correlation spectroscopy of GFP fusion proteins in living plant cells. *Methods in Enzymology*, **361**: p. 93-112.

Hink, M.A., A. van Hoek and A.J.W.G. Visser. (1999). Dynamics of phospholipid molecules in micelles: Characterization with fluorescence correlation spectroscopy and time-resolved fluorescence anisotropy. *Langmuir*, **15**(4): p. 992-997.

Howbrook, D.N., A.M. van der Valk, O.S. MC, D.K. Sarker, S.C. Baker and A.W. Lloyd. (2003). Developments in microarray technologies. *Drug Discovery Today*, **8**(14): p. 642-651.

Jacobson, S.C., M.A. McClain, C.T. Culbertson and J.M. Ramsey, *Microfabricated fluidic devices for cellular assays*, in *Micro Total Analysis Systems 2000*, vol: A. van den Berg, W. Olthuis, and P. Bergveld, Editors. 2000, Kluwer Academic Publishers. p. 107-110.

Jacobson, S.C. and J.M. Ramsey. (1997). Electrokinetic focusing in microfabricated channel structures. *Analytical Chemistry*, **69**(16): p. 3212-3217.

Janasek, D., J. Franzke and A. Manz. (2006). Scaling and the design of miniaturized chemical-analysis systems. *Nature*, **442**(7101): p. 374-380.

Jespers, L.S., J.H. Messens, A. De Keyser, D. Eeckhout, I. Van Den Brande, Y.G. Ganseman, M.J. Lauwereys, G.P. Vlasuk and P.E. Stanssens. (1995). Surface expression and ligand-based selection of cDNAs fused to filamentous phage gene VI. *Biotechnology*, **13**(4): p. 378-382.

Karlova, R., S. Boeren, E. Russinova, J. Aker, V. J and S. de Vries. (2006). The Arabidopsis SOMATIC EMBRYOGENESIS RECEPTOR-LIKE KINASE1 protein complex includes BRASSINOSTEROID-INSENSITIVE1. *Plant Cell*, **18**(3): p. 626-638.

Kask, P., R. Gunther and P. Axhausen. (1997). Statistical accuracy in fluorescence fluctuation experiments. *European Biophysics Journal*, **25**(3): p. 163-169.

Kask, P., K. Palo, N. Fay, L. Brand, U. Mets, D. Ullmann, J. Jungmann, J. Pschorr and K. Gall. (2000). Two-dimensional fluorescence intensity distribution analysis: Theory and applications. *Biophysical Journal*, **78**(4): p. 1703-1713.

Kask, P., K. Palo, D. Ullmann and K. Gall. (1999). Fluorescence-intensity distribution analysis and its application in biomolecular detection technology. *Proceedings of the National Academy of Sciences of the USA*, **96**(24): p. 13756-13761.

Kim, S.A. and P. Schwille. (2003). Intracellular applications of fluorescence correlation spectroscopy: prospects for neuroscience. *Current Opinion in Neurobiology*, **13**: p. 583-590.

Kitano, H. (2002). Systems biology: A brief overview. *Science*, **295**(5560): p. 1662-1664.

Kleber Janke, T., R. Crameri, S. Scheurer, S. Vieths and W.M. Becker. (2001). Patient-tailored cloning of allergens by phage display: Peanut (*Arachis hypogaea*) profilin, a food allergen derived from a rare mRNA. *Journal of Chromatography B*, **756**(1-2): p. 295-305.

Knight, J.B., A. Vishwanath, J.P. Brody and R.H. Austin. (1998). Hydrodynamic focusing on a silicon chip: Mixing nanoliters in microseconds. *Physical Review Letters*, **80**(17): p. 3863-3866.

Koltermann, A., U. Kettling, J. Bieschke, T. Winkler and M. Eigen. (1998). Rapid assay processing by integration of dual-color fluorescence cross-correlation spectroscopy: High throughput screening for enzyme activity. *Proceedings of the National Academy of Sciences of the USA*, **95**(4): p. 1421-1426.

Krogan, N.J., G. Cagney, H.Y. Yu, G.Q. Zhong, X.H. Guo, A. Ignatchenko, J. Li, S.Y. Pu, N. Datta, A.P. Tikuisis, T. Punna, J.M. Peregrin Alvarez, M. Shales, X. Zhang, M. Davey, M.D. Robinson, A. Paccanaro, J.E. Bray, A. Sheung, B. Beattie, D.P. Richards, V. Canadien, A. Lalev, F. Mena, P. Wong, A. Starostine, M.M. Canete, J. Vlasblom, S. Wu, C. Orsi, S.R. Collins, S. Chandran, R. Haw, J.J. Rilstone, K. Gandi, N.J. Thompson, G. Musso, P. St Onge, S. Ghanny, M.H.Y. Lam, G. Butland, A.M. Altaf Ui, S. Kanaya, A. Shilatifard, O.S. E, J.S. Weissman, C.J. Ingles, T.R. Hughes, J. Parkinson, M. Gerstein, S.J. Wodak, A. Emili and J.F. Greenblatt. (2006). Global landscape of protein complexes in the yeast *Saccharomyces cerevisiae*. *Nature*, **440**(7084): p. 637-643.

Kunst, B.H., A. Schots and A.J.W.G. Visser. (2002). Detection of flowing fluorescent particles in a microcapillary using fluorescence correlation spectroscopy. *Analytical Chemistry*, **74**(20): p. 5350-5357.

Lakowicz, J.R. *Principles of fluorescence spectroscopy*. 2 ed. Chapter 1. 1999, New York: Kluwer Academic/Plenum publishers.

Larocca, D. and A. Baird. (2001). Receptor-mediated gene transfer by phage-display vectors: applications in functional genomics and gene therapy. *Drug Discovery Today*, **6**(15): p. 793-801.

Lee, Y.H., R.G. Maus, B.W. Smith and J.D. Winefordner. (1994). Laser-induced fluorescence detection of a single molecule in a capillary. *Analytical Chemistry*, **66**: p. 4142-4149.

Lenne, P.F., D. Colombo, H. Giovannini and H. Rigneault. (2002). *Single Molecules*, **3**: p. 194-200.

Levi, V., Q. Ruan, K. Kis Petikova and E. Gratton. (2003). Scanning FCS, a novel method for three-dimensional particle tracking. *Biochemical Society Transactions*, **31**(5): p. 997-1000.

Li, H.T., L.M. Ying, J.J. Green, S. Balasubramanian and D. Klenerman. (2003). Ultrasensitive coincidence fluorescence detection of single DNA molecules. *Analytical Chemistry*, **75**(7): p. 1664-1670.

Licitra, E.J. and J.O. Liu. (1996). A three-hybrid system for detecting small ligand-protein receptor interactions. *Proceedings of the National Academy of Sciences of the USA*, **93**(23): p. 12817-12821.

Lyon, W.A. and S.M. Nie. (1997). Confinement and detection of single molecules in submicrometer channels. *Analytical Chemistry*, **69**(16): p. 3400-3405.

Magde, D., E.L. Elson and W.W. Webb. (1972). Thermodynamic fluctuations in a reacting system: measurement by fluorescence correlation spectroscopy. *Physical Review Letters*, **29**: p. 705-711.

Magde, D., E.L. Elson and W.W. Webb. (1974). Fluorescence correlation spectroscopy. II. An experimental realization. *Biopolymers*, **13**: p. 29-61.

Magde, D., W.W. Webb and E.L. Elson. (1978). Fluorescence correlation spectroscopy. III. Uniform translation and laminar flow. *Biopolymers*, **17**: p. 377-412.

Mathis, H.P., G. Kalusche, B. Wagner and J.S. McCaskill. (1997). Steps towards spatially resolved single molecule detection in solution. *Bioimaging*, **5**: p. 116-128.

McClain, M.A., C.T. Culbertson, S.C. Jacobson and J.M. Ramsey. (2001). Flow cytometry of Escherichia coli on microfluidic devices. *Analytical Chemistry*, **73**(21): p. 5334-5338.

Meldrum, D.R. and M.R. Holl. (2002). Microscale bioanalytical systems. *Science*, **297**(5584): p. 1197-1198.

Mijatovic, D., J.C.T. Eijkel and A. van den Berg. (2005). Technologies for nanofluidic systems: top-down vs. bottom-up - a review. *Lab on a Chip*, **5**(5): p. 492-500.

Mitchell, P. (2001). Microfluidics - downsizing large-scale biology. *Nature Biotechnology*, **19**(8): p. 717-721.

Müller, T., G. Gradl, S. Howitz, S. Shirley, T. Schnelle and G. Fuhr. (1999). A 3-D microelectrode system for handling and caging single cells and particles. *Biosensors and Bioelectronics*, **14**(3): p. 247-256.

Nie, S., D.T. Chiu and R.N. Zare. (1995). Real-time detection of single molecules in solution by confocal fluorescence microscopy. *Analytical Chemistry*, **67**: p. 2849-2857.

Nie, S.M. and R.N. Zare. (1997). Optical detection of single molecules. *Annual Review of Biophysics and Biomolecular Structure*, **26**: p. 567-596.

Oehlenschläger, F., P. Schwille and M. Eigen. (1996). Detection of HIV-1 RNA by nucleic acid sequence-based amplification combined with fluorescence correlation spectroscopy. *Proceedings of the National Academy of Sciences of the USA*, **93**(23): p. 12811-12816.

Pabit, S.A. and S.J. Hagen. (2002). Laminar-flow fluid mixer for fast fluorescence kinetics studies. *Biophysical Journal*, **83**(5): p. 2872-2878.

Pepperkok, R. and J. Ellenberg. (2006). High-throughput fluorescence microscopy for systems biology. *Nature Reviews Molecular Cell Biology*, **7**: p. 690-696.

Pohl, H. *Dielectrophoresis*. 1978, New York: Cambridge University Press.

Pollack, L., M.W. Tate, N.C. Darnton, J.B. Knight, S.M. Gruner, W.A. Eaton and R.H. Austin. (1999). Compactness of the denatured state of a fast-folding protein measured by submillisecond small-angle x-ray scattering. *Proceedings of the National Academy of Sciences of the USA*, **96**(18): p. 10115-10117.

Pope, A.J., U.M. Haupts and K.J. Moore. (1999). Homogeneous fluorescence readouts for miniaturized high-throughput screening: theory and practice. *Drug Discovery Today*, **4**(8): p. 350-362.

Pozrikidis, C. *Fluid Dynamics: Theory, Computation, and Numerical Simulation*. 2001, Dordrecht, The Netherlands: Kluwer Academic Publishers Group.

Prins, M.W.J., W.J.J. Welters and J.W. Weekamp. (2001). Fluid control in multichannel structures by electrocapillary pressure. *Science*, **291**(5502): p. 277-280.

Quake, S.R. and A. Scherer. (2000). From micro- to nanofabrication with soft materials. *Science*, **290**(5496): p. 1536-1540.

Resnick, R., D. Halliday and K.S. Krane. *Physics*. 4 ed. Vol. I. 1992, Toronto, Canada: John Wiley & Sons, INC.

Reyes, D.R., D. Iossifidis, P.A. Auroux and A. Manz. (2002). Micro total analysis systems. 1. Introduction, theory, and technology. *Analytical Chemistry*, **74**(12): p. 2623-2636.

Rigaut, G., A. Shevchenko, B. Rutz, M. Wilm, M. Mann and B. Seraphin. (1999). A generic protein purification method for protein complex characterization and proteome exploration. *Nature Biotechnology*, **17**(10): p. 1030-1032.

Rigler, R. (1995). Fluorescence correlations, single molecule detection and large number screening. Applications in biotechnology. *Journal of Biotechnology*, **41**: p. 177-186.

Rigler, R. and E.L. Elson, editors. *Fluorescence Correlation Spectroscopy. Theory and Applications.* 2001: Springer, Berlin.

Rigler, R., U. Mets, J. Widengren and P. Kask. (1993). Fluorescence correlation spectroscopy with high count rate and low background: analysis of translational diffusion. *European Biophysical Journal*, **22**: p. 169-75.

Rigler, R., J. Widengren and U. Mets, Interactions and kinetics of single molecules as observed by fluorescence correlation spectroscopy, in *Fluorescence Spectroscopy. New Methods and Applications*, vol: O.S. Wolfbeis, Editor. 1991, Springer-Verlag: Berlin. p. 13-24.

Rudiger, M., U. Haupts, K.J. Moore and A.J. Pope. (2001). Single-molecule detection technologies in miniaturized high throughput screening: Binding assays for G protein-coupled receptors using fluorescence intensity distribution analysis and fluorescence anisotropy. *Journal of Biomolecular Screening*, **6**(1): p. 29-37.

Sauer, M., B. Angerer, W. Ankenbauer, Z. Foldes Papp, F. Gobel, K.T. Han, R. Rigler, A. Schulz, J. Wolfrum and C. Zander. (2001). Single molecule DNA sequencing in submicrometer channels: state of the art and future prospects. *Journal of Biotechnology*, **86**(3) Special Iss. SI): p. 181-201.

Schrum, D.P., C.T. Culbertson, S.C. Jacobson and J.M. Ramsey. (1999). Microchip flow cytometry using electrokinetic focusing. *Analytical Chemistry*, **71**(19): p. 4173-4177.

Schwalbach, G., A.P. Sibler, L. Choulier, F. Deryckere and E. Weiss. (2000). Production of fluorescent single-chain antibody fragments in *Escherichia coli*. *Protein Expression and Purification*, **18**(2): p. 121-132.

Shanmugavelu, M., A.R. Baytan, J.D. Chesnut and B.C. Bonning. (2000). A novel protein that binds juvenile hormone esterase in fat body tissue and pericardial cells of the tobacco hornworm *Manduca sexta L. Journal of Biological Chemistry*, **275**(3): p. 1802-1806.

Sioud, M., M. Hansen and A. Dybwad. (2000). Profiling the immune responses in patient sera with peptide and cDNA display libraries (Review). *International Journal of Molecular Medicine*, **6**(2): p. 123-128.

Stathopoulos, C., G. Georgiou and C.F. Earhart. (1996). Characterization of *Escherichia coli* expressing an Lpp'OmpA(46-159)-PhoA fusion protein localized in the outer membrane. *Applied Microbiology and Biotechnology*, **45**(1-2): p. 112-119.

Suter, B., D. Auerbach and I. Stagljar. (2006). Yeast-based functional genomics and proteomics technologies: the first 15 years and beyond. *Biotechniques*, **40**(5): p. 625-644.

Sutera, S.P. (1993). The history of Poiseulle's law. *Annual Review of Fluid Mechanics*, **25**: p. 1-19.

Svoboda, K. and S.M. Block. (1994). Biological applications of optical forces. *Annual review of biophysics and biomolecular structure*, **23**: p. 247-285.

Thompson, N.L., Fluorescence correlation spectroscopy., in *Topics in Fluorescence Spectroscopy.*, vol: 1; J.R. Lakowicz, Editor. 1991, Plenum Press, New York. p. 337-378.

Tsien, R.Y. (1998). The green fluorescent protein. *Annual Review of Biochemistry*, **67**: p. 509-544.

Tung, Y.C., M. Zhang, C.T. Lin, K. Kurabayashi and S.J. Skerlos. (2004). PDMS-based opto-fluidic micro flow cytometer with two-color, multi-angle fluorescence detection capability using PIN photodiodes. *Sensors and Actuators B: Chemical*, **98**(2-3): p. 356-367.

Turk, B.E. and L.C. Cantley. (2003). Peptide libraries: at the crossroads of proteomics and bioinformatics. *Current Opinion in Chemical Biology*, **7**(1): p. 84-90.

Unger, M.A., H.P. Chou, T. Thorsen, A. Scherer and S.R. Quake. (2000). Monolithic microfabricated valves and pumps by multilayer soft lithography. *Science*, **288**(5463): p. 113-116.

van Criekinge, W. and R. Beyaert. (1999). Yeast Two-Hybrid: State of the Art. *Biological Procedures Online*, **2**(1): p. 1-38.

Visser, A.J.W.G. and M.A. Hink. (1999). New perspectives of fluorescence correlation spectroscopy. *Journal of Fluorescence*, **9**(1): p. 81-87.

Visser, N.V., M.A. Hink, J.W. Borst, G.N.M. van der Krogt and A.J.W.G Visser. (2002). Circular dichroism spectroscopy of fluorescent proteins. *FEBS Letters*, **521**(1-3): p. 31-35.

Voldman, J., M.L. Gray, M. Toner and M.A. Schmidt. (2002). A microfabrication-based dynamic array cytometer. *Analytical Chemistry*, **74**(16): p. 3984-3990.

Weichel, M., P. Schmid Grendelmeier, C. Rhyner, G. Achatz, K. Blaser and R. Crameri. (2003). Immunoglobulin E-binding and skin test reactivity to hydrophobin HCh-1 from *Cladosporium herbarum*, the first allergenic cell wall component of fungi. *Clinical and Experimental Allergy*, **33**(1): p. 72-77.

Wensink, H., H.V. Jansen, J.W. Berenschot and M.C. Elwenspoek. (2000). Mask materials for powder blasting. *Journal of Micromechanics and Microengineering*, **10**(2): p. 175-180.

Wensink, H., S. Schlautmann, M.H. Goedbloed and M.C. Elwenspoek. (2002). Fine tuning the roughness of powder blasted surfaces. *Journal of Micromechanics and Microengineering*, **12**(5): p. 616-620.

Widengren, J., Ü. Mets and R. Rigler. (1995). Fluorescence correlation spectroscopy of triplet states in solution: A theoretical and experimental study. *Journal of Physical Chemistry*, **99**: p. 13368-79.

Widengren, J. and R. Rigler. (1998). Fluorescence correlation spectroscopy as a tool to investigate chemical reactions in solutions and on cell surfaces. *Cellular and Molecular Biology*, **44**(5): p. 857-879.

Winkler, T., U. Kettling, A. Koltermann and M. Eigen. (1999). Confocal fluorescence coincidence analysis: An approach to ultra high-throughput screening. *Proceedings of the National Academy of Sciences of the USA*, **96**(4): p. 1375-1378.

Wölke, J. and D. Ullmann. (2001). Miniaturized HTS technologies - uHTS. *Drug Discovery Today*, **6**(12): p. 637-645.

Wright, W.H., G.J. Sonek and M.W. Berns. (1994). Parametric study of the forces on microspheres held by optical tweezers. *Applied Optics*, **33**(9): p. 1735-1748.

Wu, R.Z., S.N. Bailey and D.M. Sabatini. (2002). Cell-biological applications of transfected-cell microarrays. *Trends in Cell Biology*, **12**(10): p. 485-488.

Yamamoto, M., Y. Kominato and F. Yamamoto. (1999). Phage display cDNA cloning of protein with carbohydrate affinity. *Biochemical and Biophysical Research Communications*, **255**(2): p. 194-199.

Yeng, H.L.L., J.J. Green, S. Balasubramanian and D. Klenerman. (2003). Ultrasensitive coincidence fluorescence detection of single DNA molecules. *Analytical Chemistry*, **75**: p. 1664-1670.

Zander, C., K.H. Drexhage, K.T. Han, J. Wolfrum and M. Sauer. (1998). Single-molecule counting and identification in a microcapillary. *Chemical Physics Letters*, **286**(5-6): p. 457-465.

Zhao, B., J.S. Moore and D.J. Beebe. (2001). Surface-directed liquid flow inside microchannels. *Science*, **291**(5506): p. 1023-1026.

Zhou, T., J.P. Aumais, X.Q. Liu, L.Y. Yu Lee and R.L. Erikson. (2003). A Role for Plk1 phosphorylation of NudC in cytokinesis. *Developmental Cell*, **5**(1): p. 127-138.

Nederlandse samenvatting

Verreweg de meeste functies in een levende cel worden uitgevoerd door eiwitten die specifiek aan andere eiwitten binden. Om deze eiwit-eiwit interacties te onderzoeken kunnen bacteriofagen worden gebruikt waarop cDNA-bibliotheken tot expressie zijn gebracht. Bacteriofagen (naar het Grieks voor bacterie-eters) zijn virussen die specifieke bacteriën aanvallen. Net zoals andere virussen zijn fagen heel eenvoudig opgebouwd met een kop en een staartstuk bestaande uit een DNA-streng die omgeven wordt door een eiwitmantel (zie figuur 4-13). Bacteriofagen infecteren een cel en maken dankbaar gebruik van de biochemie van de gastheer om hun eigen bouwstenen aan te maken. Uiteindelijk overleeft de bacteriecel niet, maar barst open en komen nieuwe faagdeeltjes vrij. Dat vermenigvuldigen gaat eenvoudig omdat de fagen bacteriën infecteren en dus in een bacteriekweek groeien. Het is dan ook niet verwonderlijk te constateren dat de toepassingen van fagen liggen in het ontwerpen van nieuwe geneesmiddelen, het maken van efficiënte enzymen en enzymremmers, het selecteren van antilichamen voor diagnostiek en nog veel meer. Laten we het menselijke immuunsysteem als voorbeeld nemen. Iedere mens heeft een heel grote verzameling van ongebruikte antilichamen. Deze zijn nodig om zich te kunnen verweren tegen vrijwel elke potentiële ziekteverwekker. Antilichamen zijn eiwitten, die bestaan uit een variabel deel en een constant deel. Het variabele deel herkent het antigeen, dat bijvoorbeeld een virus kan zijn of een andere lichaamsvreemde verbinding. Het variabele deel zorgt ook voor de specificiteit van antilichamen. De totale hoeveelheid verschillende antilichamen bestaat uit ongeveer 10 miljard exemplaren. Die grote verzameling moet je zien als een bibliotheek van antilichamen. Met moleculair biologische technieken kun je het variabele deel van die antistoffen tentoonstellen op fagen; dit heet faag-display (display betekent tentoonstelling in het Nederlands). Voor faag-display wordt DNA dat codeert voor een antilichaam geplakt aan het faag DNA dat codeert voor een eiwit aan de buitenkant van de faag. Op die manier wordt het antilichaam aan de buitenkant van de faag tentoongesteld. In werkelijkheid wordt het DNA van miljarden antilichamen op miljarden fagen tegelijkertijd gebruikt. Iedere faag heeft dus 1 uniek antilichaam, en de verzameling fagen is als het ware een bibliotheek van 10 miljard verschillende antilichamen. We zijn echter slechts in enkele specifieke exemplaren geïnteresseerd, die op een slimme manier er uit gevist moeten worden. De faag-display bibliotheek ondergaat verschillende selectieronden zodat we de gevraagde antilichamen krijgen.

Faag-display bestaat meestal uit rondes met negatieve en positieve selectie en vele wasstappen. Eerst wordt negatief geselecteerd: fagen worden toegevoegd in een klein reageerbuisje waar van alles in zit. Fagen die aspecifiek binden aan het aanwezige celmateriaal worden gescheiden van de niet-bindende fagen. De niet-bindende fagen worden overgebracht naar een ander reageerbuisje voor positieve selectie. In dat buisje zit bijvoorbeeld een specifieke binder. Weer worden de niet-bindende fagen eruit gehaald, maar nu wordt verder gegaan met fagen die wel binden en dus in de reageerbuis blijven zitten. De positief geselecteerde fagen worden opgekweekt in bacteriën om weer grotere aantallen fagen te krijgen. Deze ronden van afwisselende negatieve en positieve selectie worden meestal 3 of 4 keer herhaald. Na de selectieronden worden de fagen uitverdund en uitgespreid over een plaat met bacteriën. Hierdoor ontstaan tal van 'plaques' die ieder afkomstig zijn van slechts een enkele faag.

Het spreekt bijna vanzelf dat het hele selectieproces in faag-display enorm tijdrovend is. Bovendien is het niet uit te sluiten dat we interessante eiwitten gaan missen waarvan de genen zelden tot expressie komen of dat we eiwitten met lagere affiniteit, die toch interessant kunnen zijn, hebben weggewassen. Daarom is het nodig om nieuwe 'high-throughput' selectiemethoden te ontwikkelen. Deze methoden zijn gebaseerd op een combinatie van gevoelige detectietechnieken en het gebruik van microtechnologie. In dit proefschrift wordt een 'proof of principle' gegeven dat deze combinatie heel goed werkt. De detectietechniek is fluorescentie, die de ultieme gevoeligheid bezit van het detecteren van letterlijk enkele moleculen, omdat die na excitatie met een laser duizenden fotonen licht kunnen uitzenden, waarvan er voldoende overblijven om in een confocale microscoop met gevoelige lichtdetectoren te registreren. De microtechnologie component bestaat uit de ontwikkeling van 'microfluidic devices' die we gemakshalve aanduiden met biochips, omdat we gebruikmaken van het meten van biochemische processen op de schaal van micrometers zoals in een computerchip (1 μm is 10^{-6} m). In de laatste jaren zijn biochips gebruikt voor vele toepassingen. In biochips zijn micrometer kanalen geëtst, die uiterst kleine hoeveelheden vloeistoffen (picoliters; 1 picoliter is 10^{-12} liter) kunnen transporteren. Een dergelijke biochip kan worden uitgebreid tot een heuse 'lab-on-a-chip' door vloeistofkanalen te combineren met pompjes, mixers, klepjes, electrische componenten, lampjes, lichtdetectoren en andere onderdelen. Deze schaalverkleining (miniaturisatie) biedt diverse voordelen ten opzichte van een laboratorium op macroschaal. Dankzij het kleine volume zijn er minder reagentia nodig zodat kosten kunnen worden bespaard. Reacties verlopen sneller doordat reagentia veel sneller met elkaar mengen. Door de gunstige oppervlakte/volume verhouding van de kanalen wordt vrijgekomen warmte efficiënt afgevoerd. Er

zijn al grote vorderingen gemaakt in de microtechnologie, niet alleen in de ontwikkeling van materialen om biochips te maken, maar ook in methoden om de vloeistof door microkanalen te laten stromen. We kunnen vloeistof laten stromen door het toepassen van druk, vacuüm of elektrische velden. In het laatste geval is elektro-osmotische stroom (EOF) een veel gebruikte manier om vloeistof te transporteren. De stroomrichting kan worden bepaald door mechanische kleppen te bedienen of door spanningsgradiënten te veranderen. Elektrisch geladen deeltjes kunnen in een stilstaande vloeistof, wanneer EOF is onderdrukt, worden voortbewogen in een DC elektrisch veld (electroforese) of in een AC veld (di-elektroforese).

De doelstelling van het onderzoek dat in dit proefschrift wordt beschreven was het ontwerpen van een 'microfluidics' platform voor het screenen van eiwitbibliotheken zoals bacteriofagen. Het onderzoek heeft uiteindelijk geleid tot een demonstratieplatform voor het sorteren van deeltjes, die kleiner zijn dan cellen, zoals fluorescent gelabelde (sub)micrometer latex bolletjes en virussen. De deeltjes mogen een relatief lage fluorescentieopbrengst hebben doordat ze langer kunnen worden geanalyseerd in de microsorteermachine dan met conventionele FACS (fluorescence activated cell sorter) apparatuur, die vele duizenden cellen per minuut kan screenen.

In hoofdstuk 2 worden capillaire vloeistofstroom experimenten beschreven met fluorescerende moleculen, bacteriën en latex bolletjes waarbij fluorescentie correlatie spectroscopie (FCS) als analytisch hulpmiddel wordt gebruikt. Een verdunde oplossing met fluorescerende deeltjes wordt door een vierkante microcapillair (lengte 100 μm) gepompt. De fluctuaties in fluorescentie-intensiteit worden gemeten in een confocale microscoop en 'real-time' gecorreleerd. Dit geeft een autocorrelatie curve, waarvan het verval wordt bepaald hoe lang het deeltje zich in het confocale volume bevindt. Het confocale volume bedraagt ongeveer 1 femtoliter (10^{-15} liter). De stroomsnelheid wordt berekend door de autocorrelatie curve te fitten met een model, dat diffusie en stroomsnelheid als parameters bevat. Het stroomprofiel van de vloeistof binnen microcapillairen kon ook worden bepaald door de autocorrelatie curve van een kleine fluorescerende kleurstof te analyseren. Het stroomprofiel had een parabolische vorm, maximale stroomsnelheid in het midden van het capillair en zeer langzaam aan de wanden. Het laserlicht veroorzaakte optische krachten waardoor de beweging van bacteriën en latex bolletjes in de vloeistofstroom enigszins werd vertraagd.

In hoofdstuk 3 worden een drietal technologieën afzonderlijk besproken met het doel om een multifunctionele microsorteermachine te ontwikkelen. De eerste technologie is die van cDNA faag-display. De expressie van cDNA

bibliotheken op bacteriofagen heeft al geleid tot isolatie van een groot aantal eiwitten met diverse functies. Ook de tweede technologie, die van de detectie van enkele moleculen door middel van fluorescentie in een confocale microscoop, heeft een hoge vlucht genomen. Hetzelfde geldt voor de microtechnologie voor het vervaardigen van biochips. De selectie van specifiek bindende moleculen zoals kleine en grote eiwitten door middel van cDNA faag-display, kan vrij tijdrovend zijn. Het is daarom wenselijk om een strategie te ontwikkelen die veel sneller in staat is om potentiële kandidaten uit cDNA bibliotheken te selecteren. Een 'high-throughput' micro-platform wordt voorgesteld dat fluorescerende componenten van een bibliotheek door microkanalen voortstuwt. De biochip is gemonteerd op de tafel van een confocale microscoop. De fotonen afkomstig van de passerende, fluorescerende deeltjes worden 'real-time' gemeten en positief bevonden deeltjes worden gesorteerd.

In hoofdstuk 4 wordt een micro-systeem beschreven voor de detectie en sortering van afzonderlijke fluorescerende deeltjes zoals latex bolletjes en virussen in een water. Het systeem bestaat uit een biochip, computergestuurde spanningsgenerator, en een confocale fluorescentiemicroscoop. De lichtdetector is een gevoelige fotodiode die enkele fotonen kan detecteren. De output van de fotodiode wordt gekoppeld aan een 'photon-burst' analyseapparaat dat 'real-time' de spanningsgenerator voor de sortering aanstuurt. Elektro-osmotische vloeistofstromen en elektrische velden zijn gebruikt om deeltjes door het observatievolume van de microscoop te leiden. De 'real-time' detectie en efficiënte sortering van fluorescerende bolletjes werden aangetoond. De biochip heeft beperkingen voor het screenen van fluorescerende bacteriofagen. Net als de bolletjes kunnen T7 bacteriofagen door microkanalen worden voortbewogen door middel van elektrische velden. Het focusseren van de bacteriofagen was niet mogelijk en is toe te schrijven aan de relatief grote breedte van het microkanaal (5-10 μm) in vergelijking tot de afmetingen van het deeltje (circa 50 nm). In een kanaal met een breedte en een diepte van 10 μm en een detectiegebied van 0.5 μm in diameter en 2-3 μm in hoogte, zullen de meeste bacteriofagen niet worden gedetecteerd. Met deze configuratie is het dus moeilijk om afzonderlijke bacteriofagen te detecteren en te sorteren.
Hoe kunnen we de deeltjessorteerder verder verbeteren om toch fagen te sorteren? Er zijn al grote vorderingen gemaakt met de fabricage van 'nanofluidic devices' die een verdere miniaturisatie tot gevolg heeft (1 nm is 10^{-9} m). Laten we een dergelijk systeem een nanobiochip noemen. Een groot voordeel van een nanobiochip is dat fluorescentie kan worden gedetecteerd zonder de deeltjesstroom te focusseren. Om een nanobiochip goed te laten werken moeten een aantal technieken en methoden verder worden ontwikkeld.

Zo moet de stroomsnelheid van de vloeistof in een nanobiochip worden geregeld. Momenteel is de sorteersnelheid van kleine deeltjes te laag voor praktisch gebruik. Indien men 10^5 – 10^6 deeltjes uit een bibliotheek wil sorteren in een kort tijdsbestek, moeten vele nanobiochips parallel worden geschakeld. Ook moeten gevoelige ruimtelijke detectiemethoden worden gebruikt zoals een 'image intensified' CCD camera of foton-detectoren die direct in de chip worden geïntegreerd. De snelheid van data analyse kan worden verbeterd door betere besturingselektronica en 'real-time' analyse software te ontwikkelen. Er moet eveneens aandacht worden besteed aan het ontwerp van fluorescente biosensoren, die een uniek ja/nee antwoord kunnen geven. Al deze ontwikkelingen zullen resulteren in een geïntegreerd systeem waarmee cDNA bibliotheken sneller kunnen worden geanalyseerd. Dit is noodzakelijk in het postgenomische tijdperk waarin een snelle vertaling van gensequenties naar genen en naar celfunctie van groot belang is. We verwerven hiermee een groter inzicht in het functioneren van eiwitmachines in de cel.

Nawoord

Beno Hendrik Kunst is op 19 november 1963 geboren te Groningen. Zijn ouders noemden hem Niek. Zijn educatie traject is kortweg als volgt te duiden. Na een MLO opleiding chemische analyse in Groningen en een studie Biotechnologie aan de Rijks Hogeschool te Groningen succesvol te hebben afgerond, is hij verhuisd naar Duitsland. Hij heeft bijna negen jaar bij het Europees Moleculair Biologisch Laboratorium (EMBL) in Hamburg gewerkt als research assistent met als specialisatie real-time Röntgen diffractie en small-angle scattering gebruikmakend van een synchrotron. Daarna is hij in de groep van Professor Dr. Ton Visser gekomen om enkelvoudige molecuul spectroscopie te gebruiken in microfluidic biochips om biobibliotheken te detecteren en te sorteren. Het proefschrift dat nu uw aandacht heeft is het resultaat van deze studie.

Wetenschap kan je tegenwoordig niet meer alleen beoefenen. Veel mensen hebben direct of indirect mee geholpen aan dit onderzoek. Ik wil graag die mensen bedanken die een steentje hebben bijgedragen aan deze studie.

Ton, als allereerste bedank ik jou voor de gelegenheid om te mogen promoveren in je internationaal hoog aangeschreven Microspectroscopie groep. Je hebt me in de gelegenheid gebracht om datgene te doen wat me erg boeit namelijk detectie van losse, enkelvoudige moleculen en kleine deeltjes met behulp van miniaturisatie in een multidisciplinaire setting. De vele discussies hebben een goede bijdrage geleverd. Ton, nogmaals van harte bedankt!

Ook wil ik STW bedanken voor het mogelijk maken van dit onderzoek. Lia Kemper (STW) wordt bedankt voor het voorbereiden van de halfjaarlijkse vergaderingen. De gebruikers commissie wil ik bedanken voor hun goede adviezen: Dr. Marcel van der Vaart (Unilever Research, Vlaardingen), Prof. Dr. Hans Hofstraat (Philips Research, Eindhoven) en Dr. Klaus Weisshart (Carl Zeiss, Jena, Duitsland).

Sacco de Vries wordt bedankt voor de goede interactie en het kritisch doorlezen van het proefschrift. Happy landings! Arjen Schots wil ik bedanken voor de samenwerking tussen onze laboratoria. In het bijzonder dank ik Hans Keller voor de bacteriofagen en de vele vruchtbare discussies.

Albert van den Berg wordt bedankt voor de mogelijkheid die hij mij heeft gegeven om chips te ‘bakken’ in de cleanroom van Mesa+. Stefan Schlautmann wordt bedankt voor de assistentie in de cleanroom.

Ik mis soms wel de levendige interactie met mijn ‘maatje’ en kamergenoot Mark Hink. Het schoolbord heeft zijn goede diensten wel bewezen. Mark, het ga je goed in die Heimat! Jan Willem Borst bedank ik voor alle hulp in het natte gedeelte van het laboratorium. De soms humoristische gesprekken en serieuze discussies met Jacques Vervoort zal ik missen. Ook wil ik Colja Laane bedanken voor de hulprijke adviezen. Hans de Rooij wordt hartelijk bedankt voor het uitwerken van mijn schetsen. Ik wil in het bijzonder mijn paranimfen José Aker en Yee Lee hartelijk bedanken. Boudewijn van Veen is een spil in het MSC. Bedankt voor de hulp bij de layout van dit proefschrift. Ook wil ik Sjef Boeren bedanken voor de inwijding in de geheimen van de massaspectroscopie. Laura van Egmond-Ausma wordt bedankt voor de goede diensten.

Verder wil ik graag de volgende personen bedanken die op de een of andere manier hebben bijgedragen tot de totstandkoming van dit boekje: Adrie Westphal, Carlo van Mierlo, Cathy Albrecht, Hans Ippel, Hans Wassink, Harold Bult, Huub Haaker, Jan Rinze Peterzon, Jacob van Otten, Jelmer Ros, Jenny Russinova, Kees-Jan Francoijs, Marco Hefti, Mark Kwaaitaal, Maarten Engel, Mamoudou Hama Dicko, Marloes Schurink, Mariëlle Moonen, Marileen Dogterom, Nina Visser, Peter Kunst, Riet Hilhorst, Robin Schoemaker, Ruchira Engel, Rumyana Karlova, Sofia Moco, Walter van Dongen, Willem van Berkel, Willy van den Berg, Yves Bollen

Daarnaast wil ik alle (oud) collega’s bedanken die ik niet persoonlijk heb genoemd voor de goede sfeer op de diverse laboratoria.

List of Publications

Kunst, B.H., A. Schots and A.J.W.G. Visser. (2002). Detection of flowing fluorescent particles in a microcapillary using fluorescence correlation spectroscopy. *Analytical Chemistry*, **74**(20): p. 5350-5357. (chapter 2).

Kunst, B.H., A. Schots and A.J.W.G. Visser. (2004). Design of a confocal microfluidic particle sorter using fluorescent photon burst detection. *Review of Scientific Instruments*, **75**(9): p. 2892-2898. (chapter 4).

Visser, A.J.W.G., B.H. Kunst, H. Keller, H. and A. Schots (2004). Towards sorting of biolibraries using single-molecule fluorescence detection techniques. *Current Pharmaceutical Biotechnology*, **5**: p. 173-179. (chapter 3)

Garidel, P., G. Förster, W. Richter, B.H. Kunst , G. Rapp and A. Blume (2000). 1,2-Dimyristoyl-sn-glycero-3-phosphoglycerol (DMPG) divalent cation complexes: an X-ray scattering and freeze-fracture electron microscopy study. *Physical Chemistry and Chemical Physics*, **2**: p. 4537-4544.

This research has been supported by the Technology Foundation STW, the applied science division of The Netherlands Organization for Scientific Research NWO and the technology program of the Ministry of Economic Affairs (Grant WBI 4797).